1.0

1.1

1.25 1.4 1.6

1.8

2.0

2.2

2.5

2.8

3.2

3.6

4.0

4.5

MICROCOPY RESOLUTION TEST CHART
NATIONAL BUREAU OF STANDARDS-1963-A

NAVAL POSTGRADUATE SCHOOL
Monterey, California

THESIS

STUDY OF COMPUTER SIMULATION OF SPUTTERING
FROM NITROGEN REACTED MOLYBDENUM
AND TUNGSTEN TARGETS

by

Lieutenant Commander Stephen McDonald Webb

June 1986

Thesis Advisor: Don E. Harrison Jr.

Approved for public release, distribution unlumited

AD-A173586

REPORT DOCUMENTATION PAGE

1a. REPORT SECURITY CLASSIFICATION	1b. RESTRICTIVE MARKINGS
Unclassified	

2a. SECURITY CLASSIFICATION AUTHORITY	3. DISTRIBUTION / AVAILABILITY OF REPORT
2b. DECLASSIFICATION / DOWNGRADING SCHEDULE	

4. PERFORMING ORGANIZATION REPORT NUMBER(S)	5. MONITORING ORGANIZATION REPORT NUMBER(S)

6a. NAME OF PERFORMING ORGANIZATION	6b. OFFICE SYMBOL (If applicable)	7a. NAME OF MONITORING ORGANIZATION
Naval Postgraduate School	33	Naval Postgraduate School

6c. ADDRESS (City, State, and ZIP Code)	7b. ADDRESS (City, State, and ZIP Code)
Monterey, California 93943-5000	Monterey, California 93943-5000

8a. NAME OF FUNDING / SPONSORING ORGANIZATION	8b. OFFICE SYMBOL (If applicable)	9. PROCUREMENT INSTRUMENT IDENTIFICATION NUMBER

8c. ADDRESS (City, State, and ZIP Code)	10. SOURCE OF FUNDING NUMBERS			
	PROGRAM ELEMENT NO.	PROJECT NO.	TASK NO.	WORK UNIT ACCESSION NO.

11 TITLE (Include Security Classification) STUDY OF COMPUTER SIMULATION OF SPUTTERING FROM NITROGEN REACTED MOLYBDENUM AND TUNGSTEN TARGETS

12 PERSONAL AUTHOR(S) WEBB, Stephen M.

13a. TYPE OF REPORT	13b. TIME COVERED	14. DATE OF REPORT (Year, Month, Day)	15. PAGE COUNT
Master's Thesis	FROM _____ TO _____	1986 June	86

16. SUPPLEMENTARY NOTATION

17	COSATI CODES		18. SUBJECT TERMS (Continue on reverse if necessary and identify by block number)
FIELD	GROUP	SUB-GROUP	Sputtering
			Computer Simulation

19 ABSTRACT (Continue on reverse if necessary and identify by block number) The Naval Postgraduate School simulation model, QDYN85, was used to investigate the sputtering of nitrogen reacted tungsten and molybdenum targets, where the nitrogen was placed in equilibrium positions both above and below the target surface plane. The cascades were initiated by bombarding the targets with argon ions with energies varying from 1 keV to 3 keV. The simulation results, when compared to experimental results obtained by Winters, indicate that the nitrogen position is not below the surface plane for either target but is located near the point where the adatom would be equidistant from its five nearest neighbors. Furthermore, the results show no multimer formation as a result of lattice fragmentation but do show dimer formation as a result of recombination above the target of individually sputtered atoms.

20. DISTRIBUTION / AVAILABILITY OF ABSTRACT	21. ABSTRACT SECURITY CLASSIFICATION
☒ UNCLASSIFIED/UNLIMITED ☐ SAME AS RPT. ☐ DTIC USERS	Unclassified

22a. NAME OF RESPONSIBLE INDIVIDUAL	22b. TELEPHONE (Include Area Code)	22c. OFFICE SYMBOL
Don E. Harrison Jr.	(408) 646-2877	61Hx

DD FORM 1473, 84 MAR 83 APR edition may be used until exhausted. SECURITY CLASSIFICATION OF THIS PAGE
All other editions are obsolete.

Study of Computer Simulation of Sputtering from Nitrogen
Reacted Molybdenum and Tungsten Targets

by

Stephen McDonald Webb
Lieutenant Commander, United States Navy
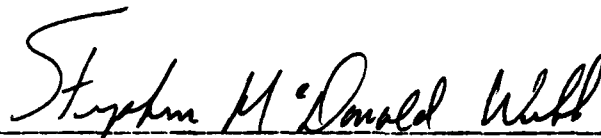B.S. University of Louisville, 1976

submitted in partial fulfillment of the
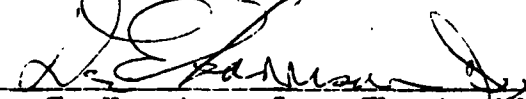requirements for the degree of

MASTER OF SCIENCE IN PHYSICS

from the

NAVAL POSTGRADUATE SCHOOL
JUNE 1986

Author: _____
Stephen McDonald Webb

Approved by: _____
Don E. Harrison Jr., Thesis Advisor

_____
Kai E. Woehler, Second Reader

_____
Gorden E. Schacher, Chairman
Department of Physics

_____
John N. Dyer, Dean of Engineering and Science

ABSTRACT

The Naval Postgraduate School simulation model, QDYN85, was used to investigate the sputtering of nitrogen reacted tungsten and molybdenum targets, where the nitrogen was placed in equilibrium positions both above and below the target surface plane. The cascades were initiated by bombarding the targets with argon ions with energies varying from 1 kev to 3 kev. The simulation results, when compared to experimental results obtained by Winters, indicate that the nitrogen position is not below the surface plane for either target but is located near the point where the adatom would be equidistant from its five nearest neighbors. Furthermore, the results show no multimer formation as a result of lattice fragmentation but do show dimer formation as a result of recombination above the target of individually sputtered atoms.

TABLE OF CONTENTS

5

ACKNOWLEDGEMENTS

I wish to thank Mr. Dirk Meyerhoff for the usage of several figures from his thesis. I would also like to thank Prof. Don E. Harrison for his guidance, patience and for keeping me on the straight and narrow without which, I could not have completed this thesis.

I. OVERVIEW

A. DEFINITION AND EARLY EXPERIMENTAL WORK

Sputtering is the ejection of surface atoms from an object due to energy transfer from an energetic projectile ion to the atoms of the object. During each collision between the energetic ion and a target atom, some energy and momentum is given up by the ion. If this transferred energy exceeds the atoms' lattice binding energy, the struck atom (recoil atom) will be displaced out of its lattice site and will collide with other target atoms initiating a cascade. If a recoil atom is located at the surface of the target, and its acquired energy exceeds the surface binding energy, and the direction of motion is away from the target, that atom will be ejected. This cascade sequence continues until the initial energy has been dissipated so far that further collisions could not possibly result in target atom displacements.

The sputtering process was first reported in 1852 by GROVE (Ref 1) when he noticed a deterioration of cathodes and a blackening of the glass of glow discharge tubes. Over the next several decades, a considerable amount of work was done in the field of sputtering. However, a lack of understanding of how various parameters such as ambient pressure, target purity and angle of incidence of the ion beam would affect the sputtering yield ,Y, (defined as the

number of ejected particles per incident ion) resulted in non-reproducible experiments. This effectively negated these early efforts.

By 1902, GOLDSTEIN (Ref 2) presented evidence that sputtering was caused by positive ions impacting on the metal cathode. Since this was considered a deterioration and thus an undesireable effect at the time, work in the area was centered on controlling the sputtering effect. However, some early researchers such as PLUCKER (Ref 3), recognized the possibilities for other experimental work of the effect in thin film manufacturing and removal. PLUCKER and other pioneers in sputtering laid the foundation which established sputtering as a field of quantitative experimental research.

B. THEORETICAL AND EXPERIMENTAL DEVELOPMENTS

The dependence of the sputtering yield on the ambient pressure was first demonstrated by PENNING and MOUBIS (Ref 4) in 1940. They realized that the number of collisions between atoms ejected from the target and atoms of the ambient atmosphere of the vacuum system increased when the pressure was increased. They showed that this was causing backscattering of sputtered atoms into the target. To overcome this effect, they kept the ambient pressure no higher than 10^{-5} Torr. At this level, reproducible results were obtained for ion energies greater than 500 ev. For ion energies less than 500 ev, the sputtering action was

8

insufficient to maintain a "clean" surface.

STARK (Ref 5), pursuing sputtering as an individual, atomic scale event, developed two separate models of the process. His hot spot model was based on the assumption that the evaporation of target material from a very small area was caused by the high temperature created by the ion's impact. VON HIPPLE (Ref 6) further developed this approach and expended a considerable amount of effort attempting to formulate a sputtering theory based on this premise, stating that this approach was the only feasible avenue to address the complex statistics of the collision processes occuring in a sputtering event. It should be noted that although this approach has recently been reexamined by KELLY and coworkers (Ref 7), it has not enjoyed the attention and development accorded to Stark's other model, the "collision" model. In 1921, KINGDON and LANGMUIR (Ref 8) produced a successful application of Stark's collision theory to the analysis of ion induced desorption of monolayers.

In the 1950's, KEYWELL (Ref 9,10) attempted to formulate Stark's collision model in terms of neutron transport theory. This and subsequent calculations by HARRISON (Ref 11) were significant because probability concepts, in the form of collision cross sections, were introduced into the theory. Although important steps, these theories were not useful because they depended on a large number of unknown parameters; so quantitative yield values could not

be calculated. In 1956, WEHNER (Ref 12) demonstrated the effect that the target's crystalline structure could have on the sputtering process when he observed spot patterns while bombarding various monocrystals. These spots were atom ejection patterns which corresponded to the close-packed directions of the monocrystal target.

Futher theoretical work by SILSBEE (Ref 13) led to the suggestion that energy was transported through a lattice structure by momentum transfer along close packed directions. This phenomenon is called focusing and the transport mechanism is called a focuson. Extensions of Silsbee's focusing concept were developed by THOMPSON (Ref 14) and by experimental work by NELSON and THOMPSON (Ref 15). While the focuson mechanism exists, subsequent investigations have shown that its contribution to sputtering is small and that, by itself, it could not explain the spot patterns observed by WEHNER. By analogy, ROBINSON and OEN (Ref 16) expected that a channelling effect on an ion through the lattice would be found. This channelling effect would, of course, be dependent on the angle of incidence and the crystalline structure. They effectivly discovered this while studying ion penetration of a crystalline structure using a simulation model. This phenomenon was confirmed later experimentally by DAVIES et al. (Ref 17)

Alternative theoretical approaches to the sputtering

10

problem culminated in the theories of SIGMUND (Ref 18) and THOMPSON (Ref 14) which consider ensemble averages over distribution functions. This approach suppresses any use of a target lattice structure in favor of an amorphous target. At higher energies, reasonably correct values of the sputtering yield, the correct form for the ejected atom energy distribution function and the ejected atom angular distribution function from polycrystalline targets are obtained. This theory is relativly inaccurate at low ion energies since it is in this region that lattice effects are most pronounced and are of significant consequence. While refinements and improvements followed, attempts to reduce a many - bodied, multiple interaction event into an analytically feasible model have still not been able to fully explain observed behavior.

C. COMPUTER SIMULATION

With the advent of high speed, sophisticated computers, it became possible to simulate a sequence of atomic collision events. The development of the simulation tool proceeded along two paths. Since the development of sputtering as a series of independent binary collisions was a natural outgrowth of STARK'S initial theories, this type of simulation was developed first. One of the principle philosophical drawbacks to this approach is that a complete understanding of the physical model is assumed and that the

assumption that each event is separate from another can be justified. While this concept may be practical for higher initial energies, it is suspect for lower energies where multiple collisions are important.

Starting in 1960, a different approach to the sputtering simulation developed. It was recognized that, particularly at low energies, a cascade could not be treated as a series of independent events. Instead, a multiple interaction (MI) procedure was required. In this type of procedure, during a specific short period of time, many atoms of the target will simultaneously affect the cascade's development. This type of simulation was introduced by GIBSON, GOLAND, MILGRAM and VINEYARD (Ref 19) when they developed a computer simulation model of the motions of copper atoms in a crystalline target after one of the atoms had been struck by an incident ion.

This time-step approach to sputtering simulation has, over the years, illuminated important aspects of the process which were masked by the ensemble averaging theories. The realizations that sputtering occurs primarily in the first three layers of the target and that focusons do not, to a great extent, affect the sputtering yield were made in this manner. This thesis will use the MI program QDYN86 to simulate the problem outlined below.

While a computer simulation can provide insight into the sputtering process, it is just that; a simulation. An

understanding of the physical situation must be attained and balanced by physics and mathematics before a simulation can be successfully achieved. Some fundamentals, such as the interatomic potential functions, are still not fully understood. In this respect, computer simulations cannot and will not supercede experimentation. They can however, provide support and explanation of observed phenomenan and, more importantly, be used as a cutting edge of science in the probing of new ideas and concepts.

D. APPLICATIONS

Sputtering simulations are not limited to monocrystalline targets. Indeed, much of the effort currently being expended lies in the arena of alloys and chemically reacted surface bombardment. Chemical reaction of the surfaces involves the introduction of an additional, different atom onto the surface of a crystalline target. This additional atom is called an adatom. The locations of these adatoms, prior to bombardment, is usually unknown, however, for various crystalline structures, anticipated locations may be described. Both tungsten and molybdenum are BCC lattice structures and the four-fold position (Fig 1) is a possible candidate, depending on the amount of coverage desired. In that location, the adatom would sit in a position between the four face atoms and a center atom such that either the forces acting on it, such as lattice and surface binding

13

energies, equalize, or it could be in a position such that the distance to it's nearest neighbors would be equal (Fig 1). Whether the adatom is more likly to be located above or below the surface plane and which of the above situations is applicable is an unanswered question for most systems.

The realization that important real world applications can be addressed in simulations has spurred their application to surface science investigations. Corrosion, the formation of oxides on the surface of a substance, can be studied. Possible solutions to its destructive effects such as adatom placement to either prohibit or slow down the introduction of the oxygen atom into the lattice can be simulated. Conversly, positioning may allow the adatom to act as a catalyst, enhancing a desired reaction.

II. OBJECTIVES

Winters (Ref 20) has conducted experiments investigating sputtering cross sections of both tungsten and molybdenum targets which have been reacted with nitrogen adatoms, when bombarded by various ions. These experiments showed that the nitrogen sputtering yield tended to increase as the atomic weight of the target atoms increased. Thus, assuming a (001) face on the target, the sputtering yield of the nitrogen adatoms was reasoned to be dominated by the mass ratio of the substrate to the adatoms. Meyerhoff (Ref 21), using a simulation model, determined that the distance between the absorbate and the substrate atoms was more significant than the mass ratio.

Both Winters and Meyerhoff assumed that the location of the nitrogen adatoms was in the four-fold position (Fig 1). Meyerhoff conducted his simulation assuming a nitrogen location slightly above the suface plane, resulting in a position of equal distance between the adatom and all five nearest-neighbors. Earlier work by Calvenna and Schmidt (Ref 22) and Adams and Germer (Ref 23) also assumed the four-fold position however, there was little regard given to target atom displacement due to the introduction of the nitrogen adatoms. Griffiths et. al. (Ref 24) incorporated this idea in a series of experiments using low energy electron diffraction (LEED). Using the observed patterns for various

coverages and primary beam energies, they were able to show that, at a fractional coverage (defined as the ratio, for a specific face of the target, of the number of adatoms to the number of substrate atoms.) of 0.5 and a surface temperature of 1000°K, the nitrogen adatoms were unstable and were rapidly absorbed into the bulk. If the coverage was reduced to approximatly 0.4, they found that temperatures up to 1100°K did not result in any further absorption. A coverage of 0.4 however, required the formation of "islands" of substrate with nitrogen adatoms on the target (Fig 2). The target used in this thesis can be interpreted as one of these "islands". To investigate this type of structure, various laser diffraction gratings were constructed and tested by Griffiths et al. A grating with a random number of nitrogen adatoms, but with an average island size of 4X4, produced a pattern similar to that observed when LEED beams were used on an actual target although the intensities of various parts of the pattern were not similar. Harrison (Ref 25) suggested that the nitrogen adatoms could be located below the surface close to an interstitial site. As stated earlier, Meyerhoff conducted his simulation assuming the equilibrium position of the nitrogen adatom above the surface plane of the substrate. This thesis will study equilibrium points both above and below the substrate surface plane.

The primary objective of this thesis is to study

sputtering from BCC crystalline targets of molybdenum and tungsten which have had nitrogen adatoms placed in different equilibrium positions, above and below the substrate surface plane for both molybdenum and tungsten targets. The incident ions will be argon of various energies.

III. Simulation Model Development

A. QDYN85

The simulation program used for this thesis research was QDYN85. This program is an MI simulation using a time step approach. Initial inputs of crystalline structure, atomic masses, potential function parameters, adatom locations, ion energies and impact point are required. Using Hamilton's equations of motion, the program initiates and develops the subsequent cascade through the crystal until the energy of the atoms is lowered to the point where no futher ejections can occur.

After the initial ion impact, position, velocity directions and energies of affected target atoms and adatoms are computed every timestep. To compute these values for every atom, every timestep, the actual program running time (cost) would be excessive. Therefore, forces are not computed on a particular target atom until it is actually hit by a moving atom. Additionally, the program maintains a listing which is updated periodically, of each atom's nearest neighbors.

For this particular simulation, the timestep is variable and is determined by a specified distance divided by the highest atomic velocity in the target. The distance choosen for this calculation is 0.1 lattice units (LU). A lattice unit is defined as one half the lattice parameter of any

cubic crystalline structure. The lattice unit was created to facilitate calculations concerning crystal structure by eliminating the need to input a large number of new variables when there is a change in the elements being studied. To determine the appropriate timestep more accurately, the rough "distance over velocity" calculation is modified by limiting factors which take into account the previous velocity thus ensuring a smoother transition in time.

Harrison and Jakas (Ref 26) present a more detailed description and analysis of the MI code of QDYN85, as well as a comparison of its results with those obtained by TRIMSP, a binary collision simulation.

B. POTENTIAL FUNCTIONS

Of critical importance to the sputtering process is the modeling of how the atoms of the crystal interact with each other. To date, no single potential function has been developed that fully and accuratly reflects every sputtering experiment. While newer potential functions may be developed or the parameters changed to fit the observed results, the basic mechanisms remain stable. Four basic potential functions are used here.

1. Born-Mayer

This is a strictly repulsive function which is considered adequate for intermediate separations. It has the

form:

$$V(r) = a \exp(-br).$$

2.<u>Moliere</u>

This is also a repulsive function but of the form:

$$V(r) = (Z_1 Z_2 e^2 / r)[0.35\exp(-0.3r/a) + 0.55\exp(-1.2r/a)$$
$$+ 0.1\exp(-6.0r/a)],$$

where "a" is the Firsov length and is calculated as follows

$$a = 0.8853a_b / (Z_1^{1/2} + Z_2^{1/2}))^{2/3},$$

where a_b is the Bohr radius. Because the Moliere function was originally intended as an approximation to the Thomas-Fermi function, it is accepted that the value obtained for "a" may be modified. This initiated a new terminology, the "modified Moliere" potential function.

3.<u>Morse</u>

The Morse is a potential function which is both attractive and repulsive depending on the separation distance "r". It has the following form

$$V(r) = D_e \exp[-2\alpha(r - r_e)] - 2D_e \exp[-\alpha(r - r_e)],$$

where D_e is the well depth, r_e is the equilibrium separation

20

of an atomic pair and alpha is a parameter controlling the shape of the well

4. Morse-Moliere

This function is a composite potential function consisting of sections of both the Morse and the Moliere functions. The two are joined together at a specific section by a cubic spline. The intersection is determined by varying the alpha and "a" parameters of the Morse and Moliere functions respectivly to obtain an intersection where the slopes are as close together as possible. The result is a smooth joining with the repulsive wall governing the collision dynamics and an attractive well which governs the sputtering.

Obviously, values obtained by these functions are dependent on the elements used for the target, adatom and the incident ion. Table 1 gives the pertinent data for the elements used in this simulation. The value a_o is the lattice parameter, B is the binding energy of nitrogen to the substrate and C is the cohesive energy.

Table 1: Natural Data for Elements Used.

	At.Mass	Structure	a_o(Å)	B(eV)	C(eV)
Mo	95.94	BCC	3.147	N/A	6.820
W	183.85	BCC	3.165	N/A	8.900
Ar	18.0	N/A	N/A	N/A	N/A
N	14.0	N/A	N/A	6.5	N/A

5. Substrate-Substrate Function

The potential function used for the crystalline

structure is a composite Morse-Moliere function. The development of the potential parameters for this interaction will be essentially the same for the substrate-adatom, substrate-ion and adatom-ion interactions described below.

As stated earlier, the alpha and the "a" values were choosen to match the respective potential graph slopes. The value of D_e was choosen so that the energy from the atoms of the lattice, measured at the center of the lattice, equaled the cohesive energy listed in table 1. The value of R_e is the nearest neighbor separation distance. The values of R_a and R_b, the spline boundaries, were determined by the final graphs of the potentials which, in turn, were dictated by the alpha and "a" values. There is also a parameter R_c which is used in the program. It's function is to limit the distance, in lattice units, over which, the force and potential calculations are made. This value is 1.71 LU except for the substrate-substrate interaction in which case R_c is 2.40 LU.

6. Adatom-Substrate Function

The parameters for this function are determined in the same manner as the substrate-substrate function with the exception of the R_e and D_e values. In this instance, the value R_e is the measured separation distance vertically between the cubic center and the adatom and D_e is the binding energy of the nitrogen atoms to the surface, 6.5eV/atom.

7. Ion-Substrate/Adatom Functions

In addition to these adatom-substrate potential functions, others must be considered. Since nitrogen has been introduced into the target, the possibility exists that, at some time, two nitrogen atoms may become neighbors or even collide. The potential function used to describe this evolution is a pure Morse function with the following experimentally determined values:

$$\alpha = 2.700 \; \overset{\circ}{A}{}^{-1},$$
$$R_e = 1.098 \; \overset{\circ}{A},$$
$$D_e = 7.373 \; eV,$$

During the simulation of a cascade, a single incident ion is injected onto the target. Since it is unlikly that the argon ion will react with the nitrogen, molybdenum or the tungsten, these potential functions are assigned as "modified" Moliere's.

The overall initial governing factors in the determination of the above values in this and the two previous sections were the desire to obtain a smooth force curve and for the minimum point of the well depth to occur when the adatom was below the surface plane. Tables 2 and 3 show the comparison between the values assuming an adatom location of 0.05 LU below the crystalline plane, and Meyerhoff's. Table 4 shows the values assuming various above

23

plane positions but incorperating the interatomic forces.

Table 2: POTENTIAL FUNCTION PARAMETERS.
(PREVIOUS)

	De(eV)	Re(Å)	∝(Å⁻¹)	MOD a	Ra(LU)	Rb(LU)
N-Mo	1.612	1.950	2.200	0.0	.910	.970
N-W	1.300	2.380	1.650	0.0	1.140	1.140
Mo-Mo	.997	2.800	1.500	0.0	.790	.830
W-W	1.335	2.849	1.200	0.0	1.830	1.900

Table 3: POTENTIAL FUNCTION PARAMETERS (NEW)
(BELOW PLANE)

	De(eV)	Re(Å)	∝(Å⁻¹)	MOD a	Ra(LU)	Rb(LU)
N-Mo	2.970	1.524	2.600	-.800	.540	.560
N-W	3.292	1.524	2.850	-.800	.650	.670
Mo-Mo	.997	2.800	1.519	0.0	.790	.830
W-W	1.335	2.894	1.200	0.0	1.120	1.130

TABLE 4: CRYSTAL POTENTIAL FUNCTION PARAMETERS
ABOVE PLANE LOCATION

LOCATION	De (eV)	Re (Å)	∝ (Å⁻¹)		MOD a	Ra (LU)	Rb (LU)
Mo-N	.380	1.600	1.950	2.150	0.0	.720	.750
Mo-N	.245	1.997	1.738	2.143	-.8	.500	.520
W-N	.487	1.712	1.960	2.320	.9	.830	.850

Figures 3-10 show the potential and force graphs
for the new values of the crystal potential function as
compared to those used previously by Meyerhoff. A review of
the force graphs using Meyerhoff's data, shows a possible
discontinuity point in the area where the splining between
the Morse and Moliere potentials occurs. It should be noted
that, at the time of the research, the effects the
interatomic forces generated would have on the final results
was not recognized. The differences are not significant.
Figures 11 through 14 show the plots for the old and new

Mo-Mo and W-W forces. Figure 15 shows the graph of the nitrogen-nitrogen potential function and figure 16 shows the graphs of the ion-adatom and the ion-substrate potential functions.

8. Vacuum Phase Potential Parameters

The probability exists that interactions above the surface of the target will occur. The potentials used for these interactions are all pure Morse. There is a paucity of data for the Mo-Mo, W-W, Mo-N and W-N systems and, as such, approximations had to be made. The values required are D_e, R_e, "omega" and "omega-x" where the later two are functions of the vibrational and rotational energy of the system. The value α is also required and is calculated, after determining D_e, as follows:

$$\alpha = (1.36116 \times 10^{-3})(\text{omega})(m/D_e)^{1/2}$$

$$m = \text{reduced mass of the system}$$

No data could be found for the Mo-Mo, W-W, Mo-N or the W-N systems. Therefore, as a compromise, using reference 27, systems were found that were as close to the investigated system as possible in reduced mass and in location on the periodic table. For Mo-Mo, Ag-Br was used and VO was substituted for Mo-N. Similar substitutions were used for the tungsten system. The N-N system was available. Table 5

25

summarizes the values used.

TABLE 5: VACUUM PHASE POTENTIAL PARAMETERS.

	De	Re		omega	omega-x
Mo-Mo	1.700	1.790	2.390	247.700	.679
N-N	5.760	3.359	1.098	2358.570	14.320
Mo-N	6.100	1.965	1.524	1020.000	4.700
W-W	3.100	1.450	2.470	308.399	.960
W-N	4.900	2.159	1.738	967.000	4.850

C. TARGET and IMPACT AREAS

The size of the target is determined by the energy of the incident ion. If the selected target size is insufficient, it is possible that, during the course of a cascade, atoms which have escaped from the sides or the bottom of the target would have caused additional sputtering to occur if the target had been larger. Such an event is called a "failure of containment". Although a large target is desirable to maximize the sputtering yield, there exists a practcal upper bound. For a given incident energy, increasing the size of the target beyond some point would waste computer resources. Therefore, a balance must be struck between the two requirements. Using a copper target bombarded with argon, it was found that a target size of 23X8X23 for an incident energy of 2 keV would provide almost complete containment.

For this size target, the introduction of 60 nitrogen adatoms, each in the four-fold position, would result in a

26

fractional coverage of .417. Figure 17 shows the (001) face for such a target. Although nitrogen is the adatom used in this thesis, other elements may be used. This could result in the adatoms occupying a different location on the target. These locations may be the two-fold (equidistant between two nearest-neighbor substrate atoms) or the A-top (directly above a substrate atom) positions (figure 18).

A total of 600 impact points on the surface were examined for each incident ion energy value. These impact points, as measured on the x and z axis, were varied about a central, pre-selected point on the target. There were two pre-selected points, (11.000, 11.000) and (13.000, 15.000) (Fig 17). The first location does not have an occupying adatom while the second does. This method results in a large number of independent runs for a specific ion energy and therefore, more accuracy in the results.

IV. RESULTS AND DISCUSSIONS

A. ANALYZING AND PLOTTING PROGRAMS

ANMOL is the analyzing program currently being used for sputtering research at the Naval Postgraduate School. The results obtained from QDYN85 are used as input with the ANMOL program formatting and tabulating the results. The output can be varied as to the depth and detail desired for a given input.

The inputs used for the ANMOL program are also those used for the program ANPLOT which will provide graphical vice tabular results. In addition to ANPLOT, the graphics program EASYPLOT was used to generate all force and potential plots.

B. HIT/NO HIT SCENARIO

As discussed previously, each simulation run was conducted with a total of 300 impact points referenced to a pre-selected point on the target surface. For this simulation, only half of the available positions contain a nitrogen adatom. Therefore, there is an equal probability of the incident ion hitting or missing an adatom. To incorperate this difference, runs, at the same ion energy, were conducted for both instances where the ion hit and did not hit a nitrogen adatom with the results being averaged together. This results in essentially a 600 point run for each energy simulated. The primary difference of the two

28

runs is that there are approximatly two to four times the number of sputtered nitrogen atoms for the hit run as there are for the no-hit run, depending on the incident ion energy.

All table listings of yield and cross sections incorperate this hit/ no-hit scenario.

C. NITROGEN RESULTS

1.Simulated cross sections and yields

The value of the sputtering yield of nitrogen can be expressed as the product of the concentration of the nitrogen adatoms in atoms per square centimeter (θ_n) and the sputtering cross section in square centimeters (σ_n). The results are in units of nitrogen atoms per ion. Figure 19 shows the experimental results of Winters for the sputtering cross section of nitrogen versus the ion energy for a variety of substrates.

The simulated concentration of the nitrogen, assuming a coverage of 0.4, was calculated to be 5.0E14 atoms/cm^2. Table 6 shows the results of the nitrogen cross sections for both molybdenum and tungsten substrates with the adatoms located 0.05 LU beneath the surface plane.

Since the adatom/substrate potential functions change for different adatom positions, different parameters must be calculated for each assumed position of the adatom to ensure equilibrium. New potential function parameters were computed

29

for various adatom positions above the plane for both the molybdenum and tungsten systems. Table 7 shows the results for the selected positions (in parentheses below the substrate type) above the plane for each system. The unit for this distance is the LU.

TABLE 6: SIMULATION NITROGEN CROSS SECTIONS
CROSS SECTION X10^{-15}(cm^2) (BELOW PLANE)

ION ENERGY	YIELD		CROSS SECTION	
(KEV)	Mo(001)	W(001)	Mo(001)	W(001)
1	.33	N/A	.66	N/A
2	.26	.29	.52	.57
3	.23	N/A	.46	N/A

TABLE 7: SIMULATION NITROGEN CROSS SECTIONS
CROSS SECTION X10^{-15} (cm^2) (ABOVE PLANE)

ION ENERGY	YIELD			CROSS SECTION		
(KEV)	Mo(001)		W(001)	Mo(001)		W(001)
	(.245	.38)	(.487)	(.245	.380)	(.487)
1	N/A	.57	.567	N/A	1.14	1.13
2	.301	.525	.450	.6	1.05	.90
3	N/A	.55	N/A	N/A	1.10	N/A

2. Nitrogen results comparison to experimental results

Figure 20 shows a comparison for the molybdenum substrate with adatom positions of 0.05 LU below the surface for the low point and 0.38 LU above the surface for the high point.

When the cross section and yield simulation results for the molybdenum target with the below plane adatom location are compared to the experimental values obtained by Winters,

30

a strong negatively sloped curve is evident rather than a slight positive slope. Also, the simulation cross section values are below the experimentally observed values. This indicates that the adatom probably is not located beneath the surface of the target. The observed cross section for the below plane nitrogen from tungsten bombarded at 2 keV was obviously low, suggesting that the adatom was not located below the surface for that system either. This observation negated the need for further runs on tungsten at this adatom position.

Figure 20 also compares the computed molybdenum results for the two previously mentioned above plane adatom locations to those obtained by Winters. With respect to the 0.38 LU position, the curves are much closer in shape, and the new points for molybdenum are now slightly above the experimental values. This seems to indicate that the assumed position of 0.38 LU above the plane was too high a location for the adatoms.

The equidistant positioning of the adatom, which was a change of 0.135 down LU from the previously examined point, resulted in a decrease in the cross section of 40%. This large change in yield for a small change in distance supports the distance dependency postulated by Meyerhoff. These results also indicate that the position of the nitrogen adatom, for a molybdenum target, is slightly above the eqidistant position. Figure 21 and shows a comparison of

the experimental values obtained for tungsten substrate and those obtained from the simulation for the "above plane" adatom location of 0.487 LU. These appear to be in fairly close agreement. However, little can be definitivly stated since only two points were evaluated for the assumed position.

3. Simulated nitrogen energy distribution

Figures 22 through 25 show the energy distribution of the sputtered nitrogen atoms for an incident energy of 2 keV. In each case, the spectrum was fairly broad. In both extreme cases, where the adatom was located at it's closest and furthest position from the surface, for both tungsten and molybdenum, a spectrum with a peak of approximaly 5 eV is evident; therefore, the choice of the substrate, when there is a large mass difference between the substrate and the adatom, appears to be of little consequence to the energy distribution of the ejected nitrogen. Additionally, the location of the adatom has little effect on it's sputtered energy. These results conflict with those obtained by Meyerhoff.

4.Simulated nitrogen ejection angles

Figure 26 is a spot pattern presentation of the polar and azmuthal angle dependence of the sputtered nitrogen adatoms. The azmuthal angle of the spot is read normally while the polar angle of a spot is plotted as the numerical value of the tangent of the polar angle. Therefore, spots further out

32

Steve has p. 33
to darken table

correspond to adatoms with larger angles of ejection as
measured from the surface normal. Little, if any, pattern
development can be seen from the graph. Table 8 lists, in
numerical format, typical polar and azmuthal angular results
for sputtered nitrogen atoms of various energies.

Table 8: Nitrogen atom souttering angles

THETA/PHI	15	30	45	60	75	90	105	120	135	150	165	180	TOTAL
5	4	4	5	3	0	0	0	0	3	5	4	4	64
15	2	4	8	9	3	8	8	3	9	8	4	2	136
25	2	11	3	4	2	4	4	2	4	3	11	5	104
35	5	5	9	6	5	7	7	5	6	9	5	5	143
45	3	6	6	5	3	3	3	3	5	6	6	3	104
55	9	5	9	8	8	6	6	8	8	9	5	9	176
65	2	2	5	2	3	3	3	3	2	5	2	2	68
75	1	0	1	3	0	3	3	0	3	1	0	1	32
85	2	0	3	2	2	1	1	2	2	3	0	2	40

ANGULAR TALLY: ENERGY > 5.0 EV

THETA/PHI	15	30	45	60	75	90	105	120	135	150	165	180	TOTAL
5	3	1	5	3	0	0	0	0	3	5	1	3	48
15	2	2	5	7	1	7	7	1	7	5	2	2	96
25	2	6	2	4	1	3	3	1	4	2	6	2	72
35	3	4	8	3	3	4	4	3	3	8	4	3	100
45	1	4	6	5	3	2	2	3	5	6	4	1	84
55	6	4	7	7	6	5	5	6	7	7	4	6	140
65	2	2	4	2	1	2	2	1	2	4	2	2	52
75	1	0	1	3	0	2	2	0	3	1	0	1	22
85	1	0	1	0	1	2	1	1	0	1	0	1	16

ANGULAR TALLY: ENERGY > 10.0 EV

THETA/PHI	15	30	45	60	75	90	105	120	135	150	165	180	TOTAL
5	1	1	2	2	0	0	0	0	2	2	1	1	24
15	1	1	3	7	0	1	1	0	7	3	1	1	52
25	1	4	1	4	0	3	3	0	4	1	4	1	52
35	2	1	4	0	3	4	4	3	0	4	1	2	56
45	1	2	4	4	1	2	2	1	5	4	2	1	60
55	5	3	6	7	5	5	5	5	7	6	3	5	124
65	2	2	3	1	0	2	2	0	1	3	2	2	40
75	1	0	1	3	2	2	2	0	3	1	0	1	28
85	1	0	1	0	1	1	1	1	0	1	0	1	16

ANGULAR TALLY: ENERGY > 20.0 EV

THETA/PHI	15	30	45	60	75	90	105	120	135	150	165	180	TOTAL
5	1	1	1	0	0	0	0	0	0	1	1	1	12
15	0	0	3	4	0	1	1	0	4	0	2	0	32
25	2	0	4	0	2	1	0	4	0	2	1		36
35	1	0	2	0	0	2	1	0	0	2	0	1	16
45	0	1	3	3	1	1	1	1	3	1	0		28
55	5	2	3	3	3	3	3	3	3	3	2	5	76
65	0	2	1	0	0	1	1	0	2	1	0		16
75	1	0	1	2	0	2	2	0	2	1	0	1	24
85	0	0	1	0	1	2	0	1	2	1	0	0	9

D. MOLYBDENUM AND TUNGSTEN RESULTS

When the incident ion impacts a target with a chemisorbed gas; target atoms as well as the adatoms are sputtered.

Clean surface targets of both molybdenum and tungsten were bombarded in the simulation with 2 keV argon ions. The number of sputtered target atoms were then compared to the number of sputtered target atoms when the target had been reacted with nitrogen. Table 9 lists these values.

TABLE 9: SUBSTRATE ATOM EJECTIONS

	CLEAN	ADATOM POSITION	
		HIGH	LOW
Mo	907	677	686
W	791	590	561

A comparison of the number of sputtered target atoms for the low and high nitrogen positions of both substrates was done. The comparison shows that although the nitrogen acts as an energy absorption mechanism, it's location is of little consequence to the ejection mechanism of the substrate material.

1. Simulation target yield

Figures 27 and 28 show the target atom yield per impact point for a 2 keV incident ion. The bottom left corner of the diagram is the selected reference point for the ion impact. Throughout the graph, the darker the point, the higher the yield for that particular point. The lighter areas of the graphs are indicative of the channelling effect for the BCC structure.

a. Simulation Target Yield Comparison to Experiment

In his experiments, Winters also calculates the ratios of the cross sections of the chemisorbed gas to the substrate material. Table 10 lists the results of the simulation as compared to the experiment. Winters used polycrystalline tungsten and molybdenum targets in his experiments while the calculations of this thesis used clean target (no adatoms) cross sections. The simulation tungsten and molybdenum concentrations were calculated to be 1.19E15 and 1.2E15 respectivly.

TABLE 10: CROSS SECTION RATIO'S WITH NITROGEN IN EQUIDISTANT POSITION

	EXPERIMENT		SIMULATION	
ION ENERGY	$\dfrac{\sigma N(W)}{\sigma W(POLY)}$	$\dfrac{\sigma N(MO)}{\sigma MO(POLY)}$	$\dfrac{\sigma N(W)}{\sigma W(CLEAN)}$	$\dfrac{\sigma N(MO)}{\sigma MO(CLEAN)}$
2	.77	.68	.41	.24

Since the simulation clean targets were bombarded with 2 keV ions only, comparisons must be restricted to that energy. The simulation cross section value for nitrogen from the molybdenum target was calculated assuming the 0.245 position for the adatom. Table 10 shows a smaller value than the experimental ratio although the nitrogen cross section ratio for experiment and simulation are both 1.33. These results, along with the previously mentioned significant yield/distance relationship indicate that the assumed positions are close to the actual adatom locations.

35

2. Simulation probabilty of ejection

Figures 29 and 30 are representitive of the probability of ejection for each of the surface atoms, in this case on the (001) face. These figures indicate how well the cascade sequence was contained by the target. The graphs show that the size of the target was generally acceptable for molybdenum but was slightly small for tungsten. This does not affect the sputtering results for either the substrate or the adatom significantly.

3. Simulation substrate ejection spot patterns

Figures 31 and 32 show typical sputtered target atom spot patterns. As with the nitrogen graph, these give graphical representations of the angles of ejection of the target atoms. The crystalline nature of the targets is readily apparent in these graphs because of the concentration of sputtered atoms along the 45°, 135°, 225°, and 315° arms. For a BCC structure, these directions correspond to the nearest neighbor directions

4. Simulation ejected substrate energy distribution

Figures 33 through 38 show typical energy distribution histograms of the sputtered target atoms. There were no apparent differences between the specific substrate results. The molybdenum results show a maximum at approximatly 5eV while the maximum for tungsten is slightly higher. These values conflict with the theoretical values which should be one half the cohesive energy; specifically, 3.41 eV for

molybdenum and 4.45 eV for tungsten. When plotted logarithimicly, both elements approximatly show the expected E^{-2} dependency at higher energies (Fig.39 through 43). Table 11 shows the slope relationship numerically with the values having been obtained from the figures mentioned.

TABLE 11: SUBSTRATE EJECTED ATOM ENERGY DISTRIBUTION SLOPES

ION ENERGY (KEV)	SUBSTRATE	ENERGY DISTRIBUTION SLOPE
3.0	MO	-1.8
1.0	W	-1.93
2.0	W	-1.94
2.0	W (clean)	-1.99
2.0	MO (clean)	-2.13

E. DIMER RESULTS

When a compound structure is bombarded, there may be an expectation that groups of two or more atoms would be sputtered off together. The results of this simulation do not show this to be the case. In many instances however, after ejection, two atoms, either substrate - substrate or substrate - adatom combine over the target. Individual ejection times of combining atoms showed differences of as much as 200 fsec, indicating that combination occured at a relativly large distance from the target. However, there were some instances when the times of ejection were separated by as little as 10 fsec for two atoms whose pre-ejection locations were within 1 LU thus indicating dimer formation almost immediatly after ejection.

V. CONCLUSIONS AND RECOMMENDATIONS

The results of the simulations, when compared to experimental results, indicate that, for nitrogen chemisorbded on the (001) face of molybdenum and tungsten targets, the location of the adatom is above the surface plane for both targets.

Nitrogen yield comparisons between the simulation and Winters experimental results indicate that the adatom position for the molybdenum target is above the equdistant position of 0.245 LU and below the 0.380 LU position. Furthermore, the simulation yield comparisons between the two positions show that there is a very strong dependency of the yield on the adatom distance from the target surface plane.

The comparison of the simulation nitrogen yield to the experimental values for the tungsten target indicate that the adatom position is near the equidistant position of 0.487 LU. However, since only two ion energy values were analyzed for this target, further investigation of the tungsten target should be conducted at different ion energies to complete the argon simulation results.

Additionally, further simulation investigation into both molybdenum and tungsten should be conducted using different bombarding ions in the same energy range as those used in this thesis. These additional simulations should be analyzed

in conjunction with the results obtained in this thesis to isolate the exact adatom locations for the targets in question.

first layer

second layer
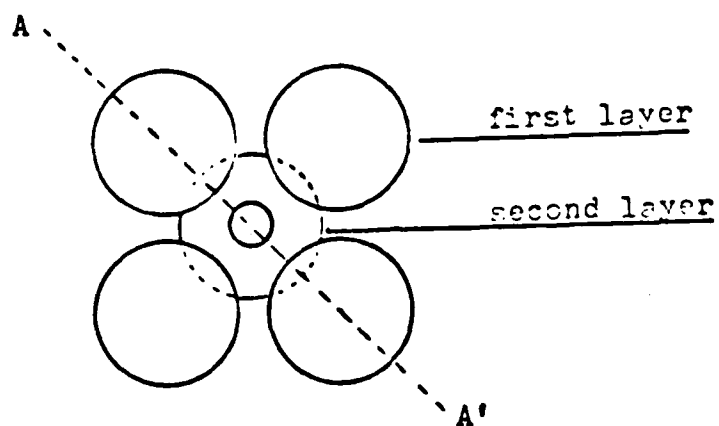
Small circle represents nitrogen atoms.

Fig. 1. Location of nitrogen atoms on target substrates

(a)

(b)
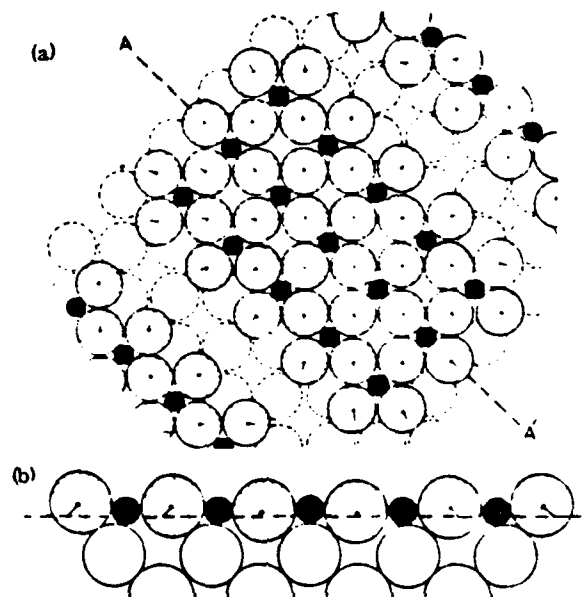
The proposed contracted-domain structure
for the 0.4 monolayer on a Mo(001) or a
W(001) surface: Large hatched circles, top-
layer substrate atoms, small filled circles
N atoms.
a) Plan view, illustrating domain and boundary
structure.
b) Cross section through the domain along AA:

Fig. 2. Island formation on a target surface

41

MO-N FORCE (PREVIOUS)
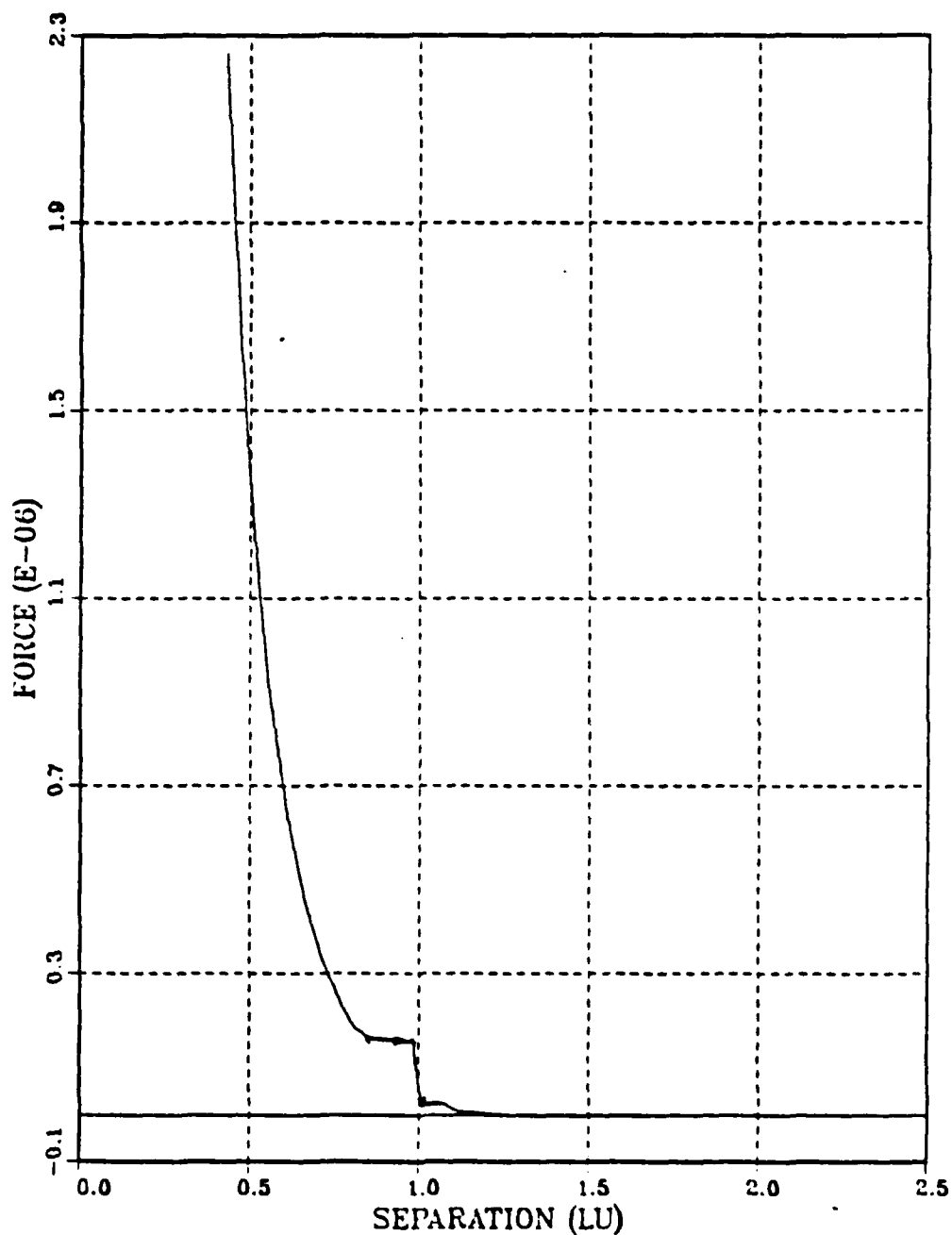
Fig. 3. Molybdenum-Nitrogen force function previously used.

MO-N FORCE (HIGH POSITION)
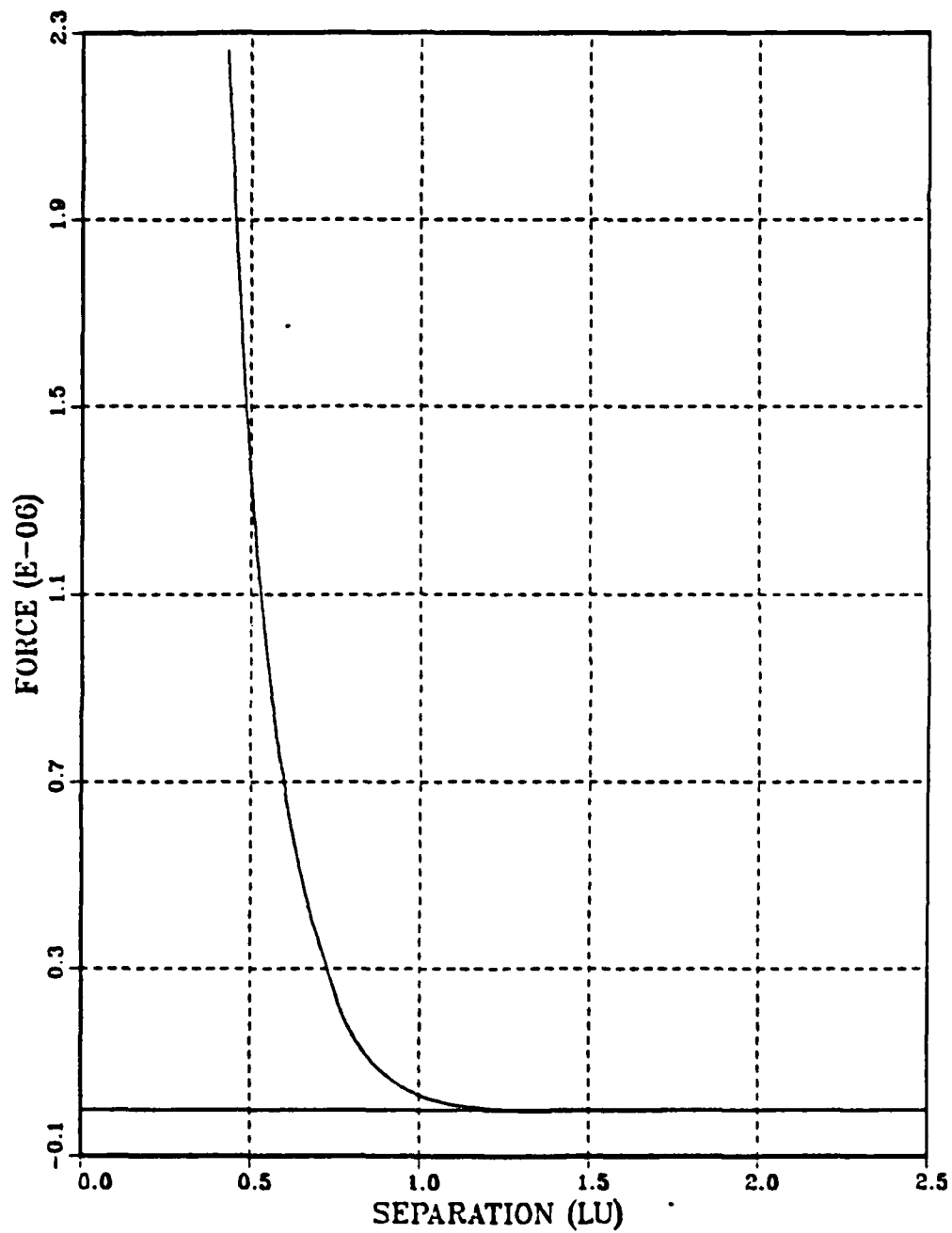
Fig. 4. Molybdenum-Nitrogen force function, adatom location 0.380 LU

MO–N FORCE (LOW POSITION)
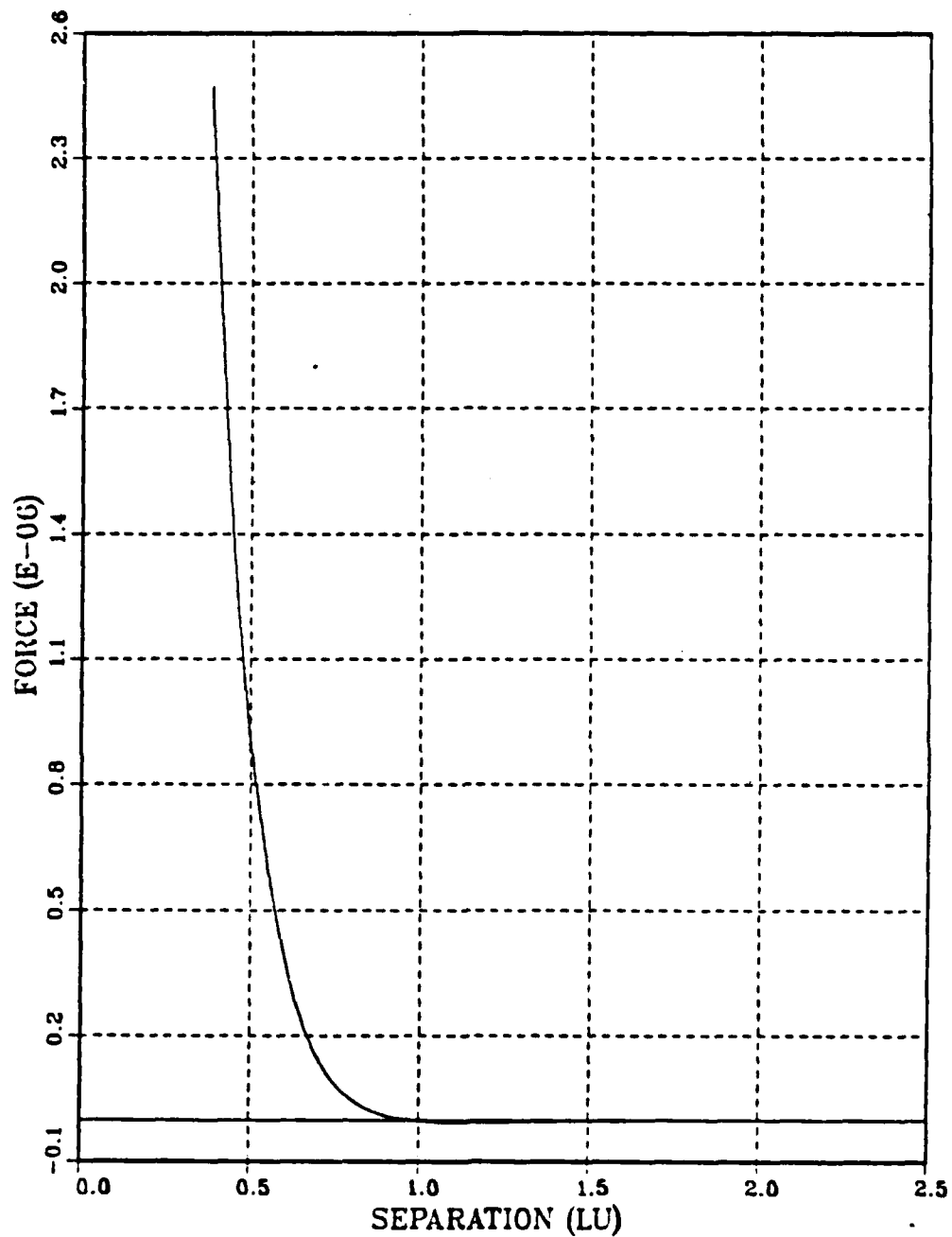
Fig. 5. Molybdenum-Nitrogen force function, adatom location
-0.05 LU

MO – MO POTENTIAL
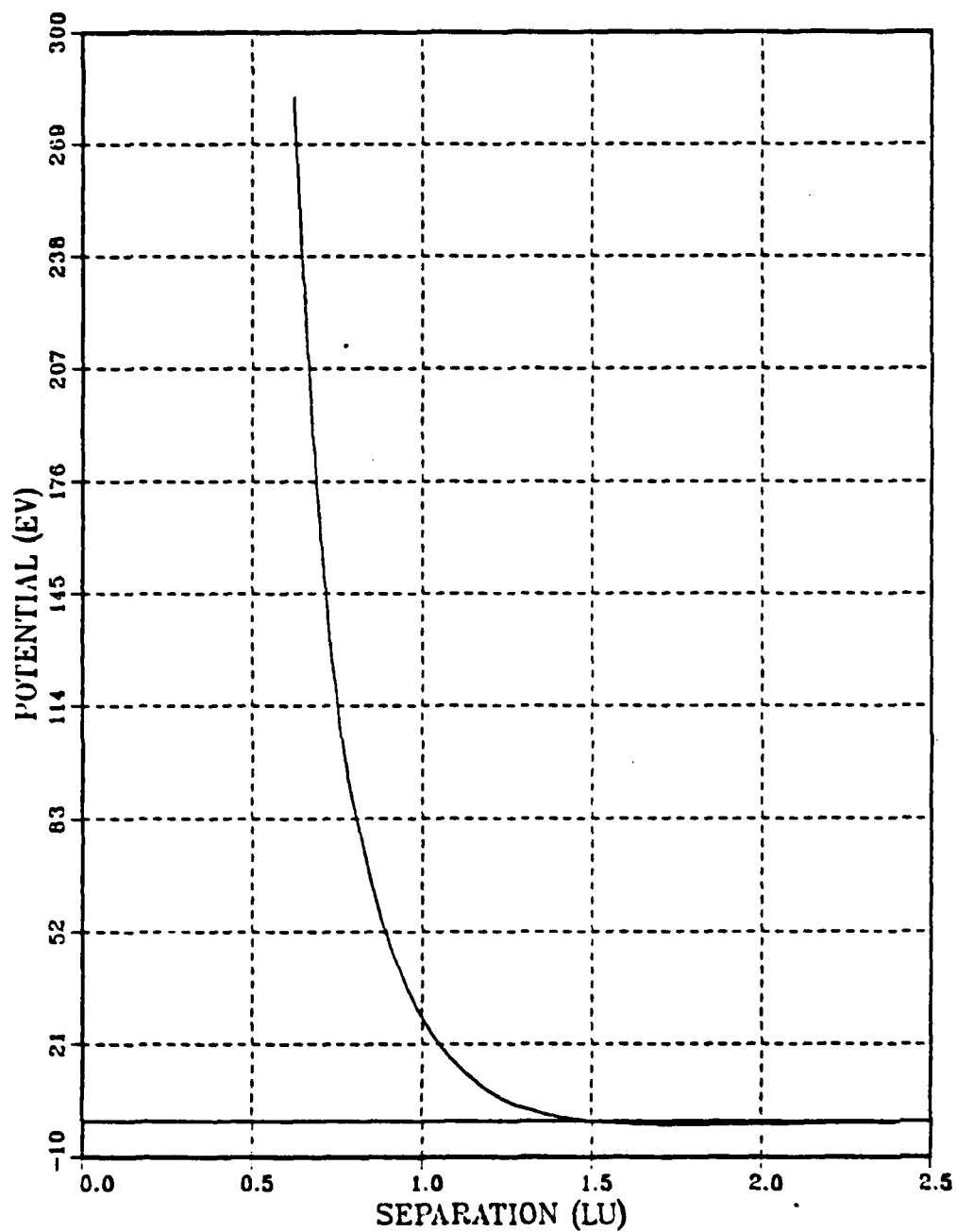
Fig. 6. Molybdenum-Molybdenum potential function

MO–N POTENTIAL
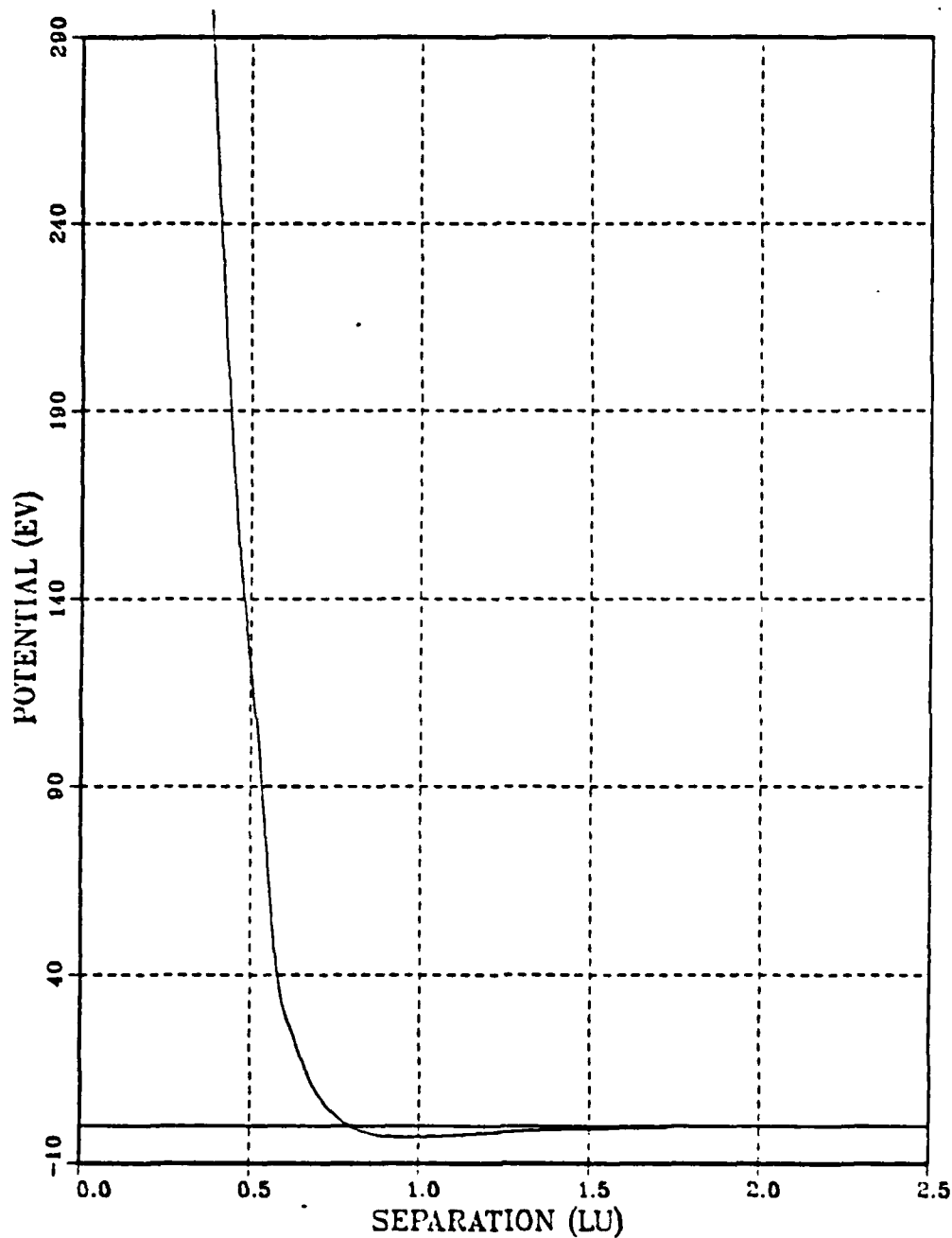
Fig. 7. Molybdenum-Nirtogen potential function

46
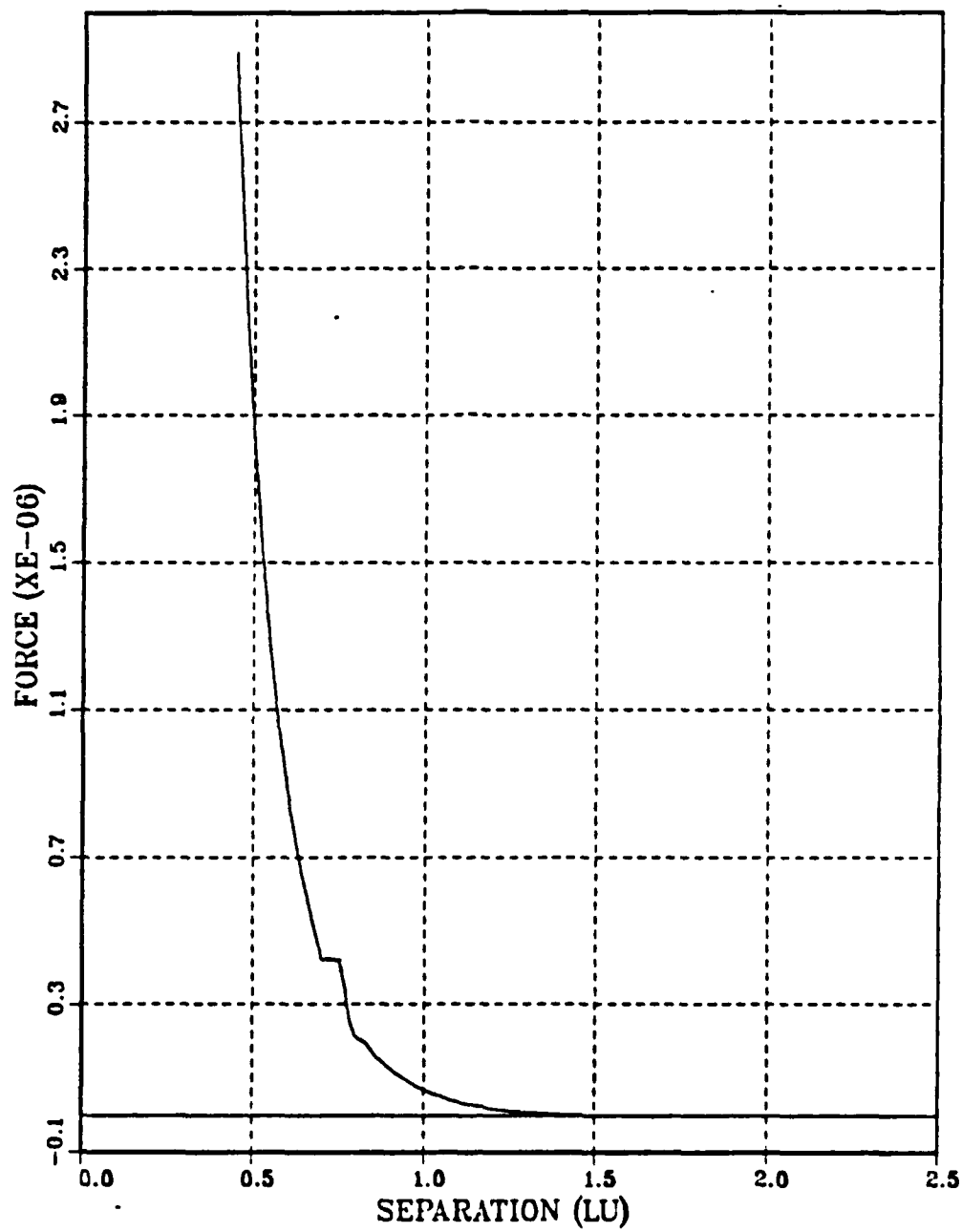
W-N FORCE (PREVIOUS)

Fig. 8. Tungsten-Nitrogen force function used previously

47
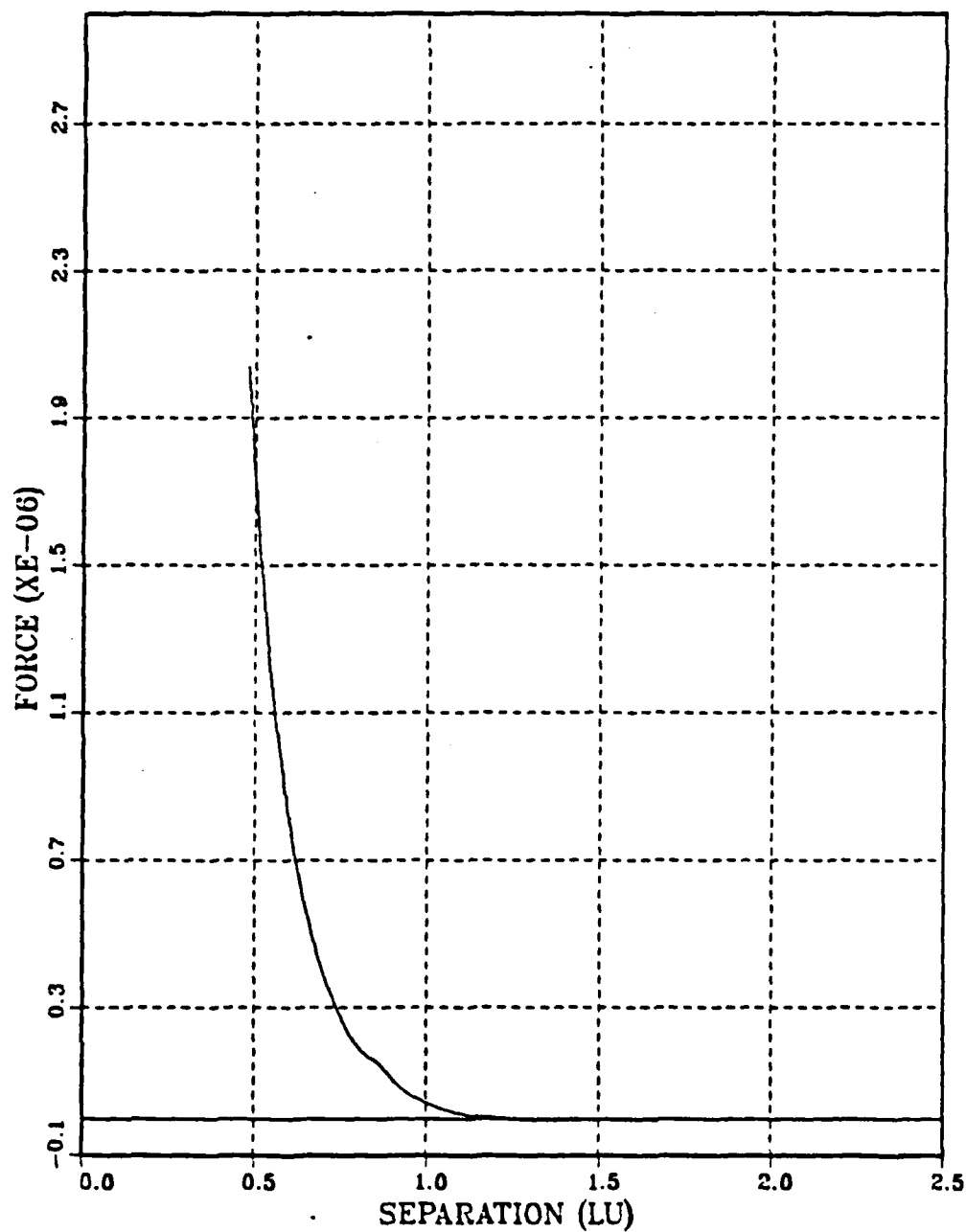
W-N FORCE

Fig. 9. Tungsten-Nitrogen force function, adatom location
0.487 LU

48
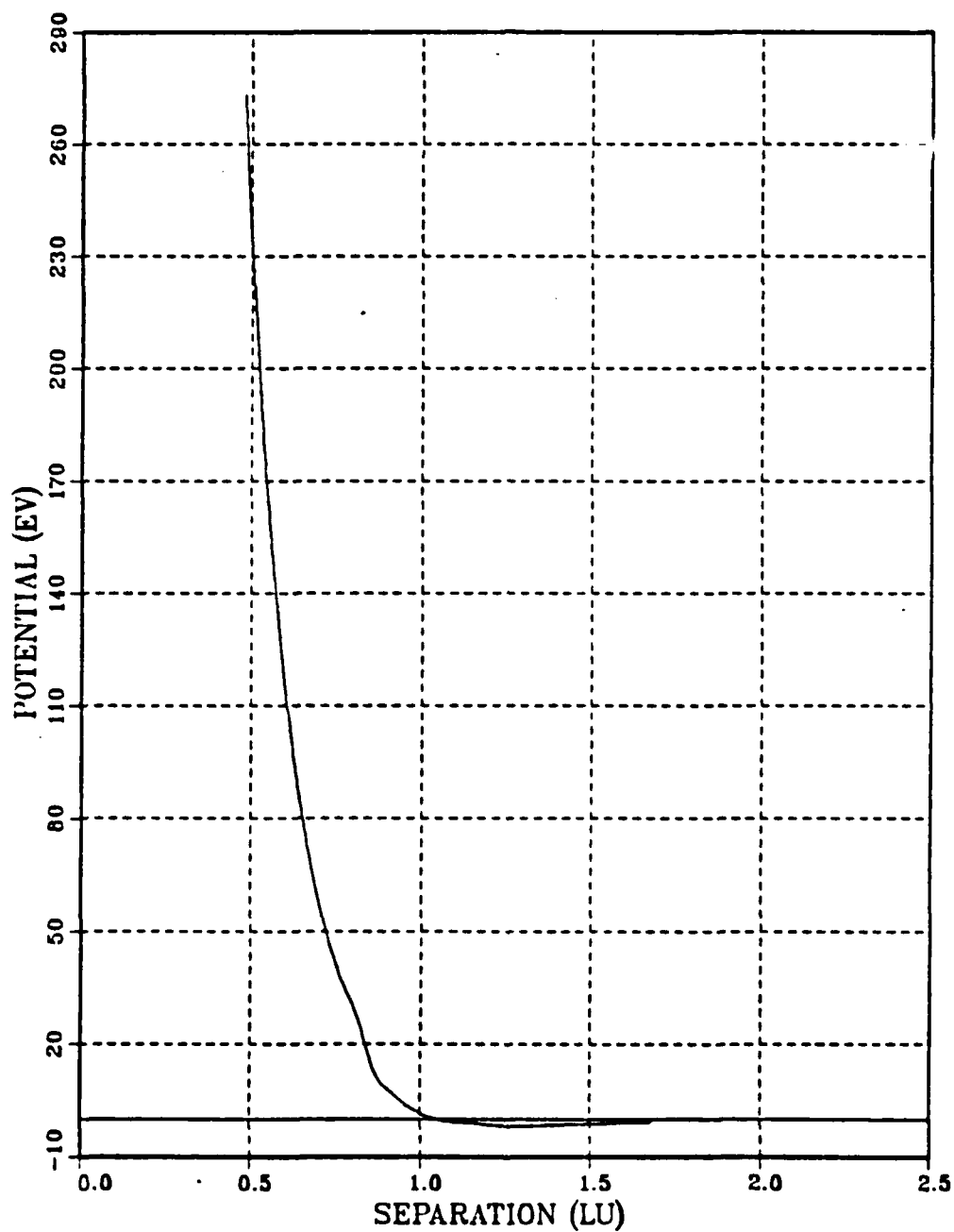
W—N POTENTIAL

Fig. 10. Tungsten-Nitrogen potential function

MO-MO FORCE (PREVIOUS)
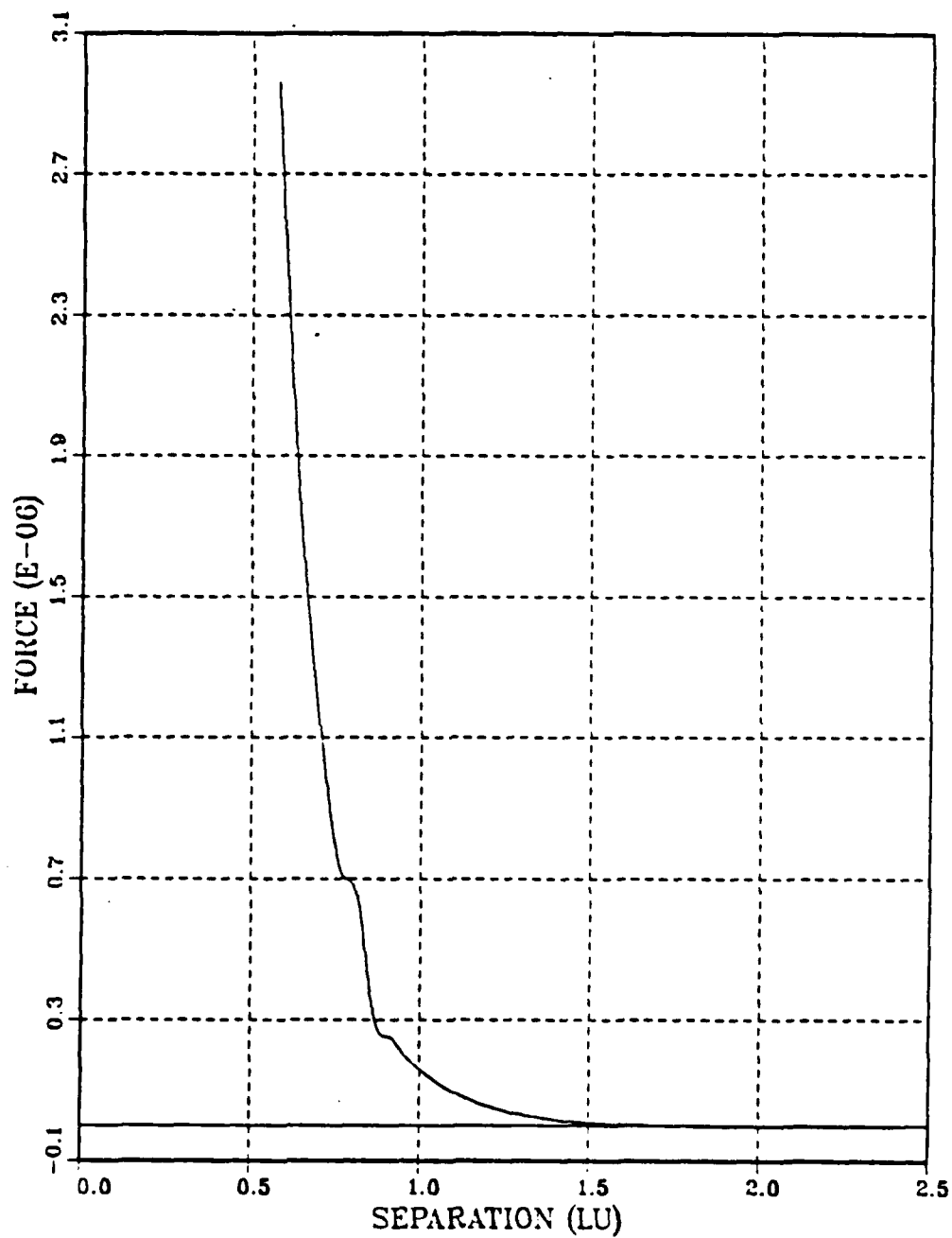
Fig. 11. Molybdenum-Molybdenum force function previously used

50

MO–MO FORCE
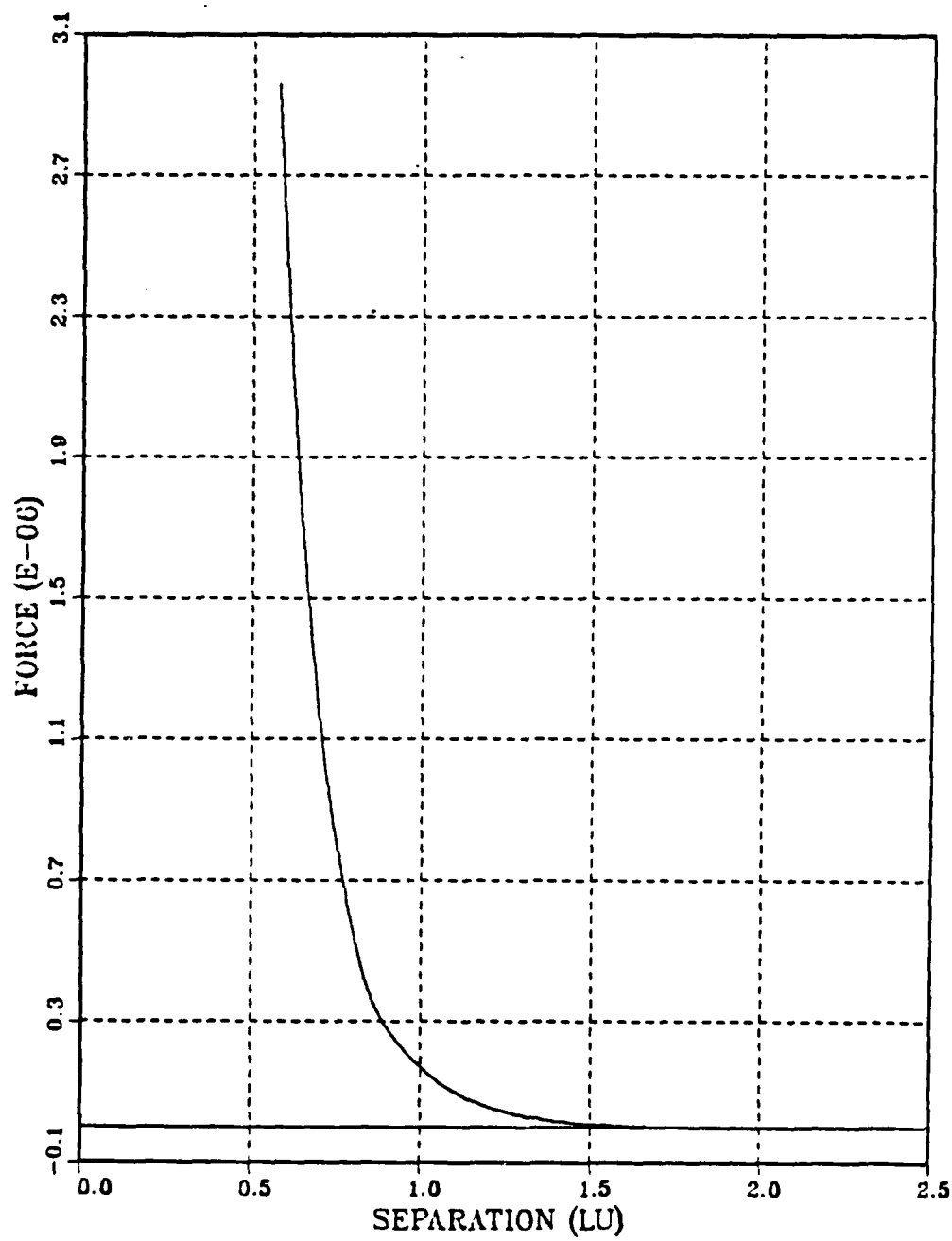
Fig. 12. Molybdenum-Molybdenum force function

W—W FORCE (PREVIOUS)
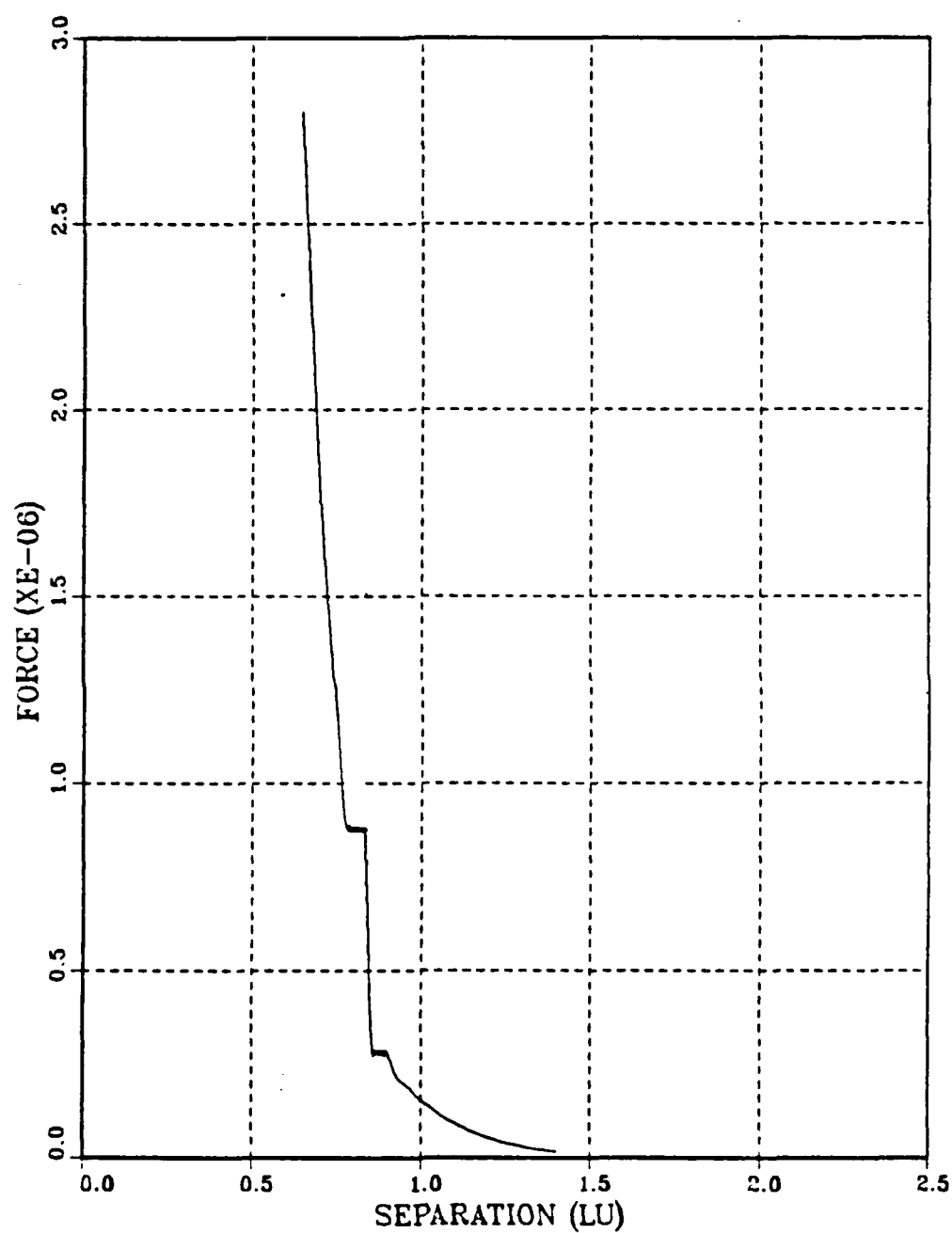
Fig. 13. Tungsten-Tungsten force function previously used

W–W FORCE
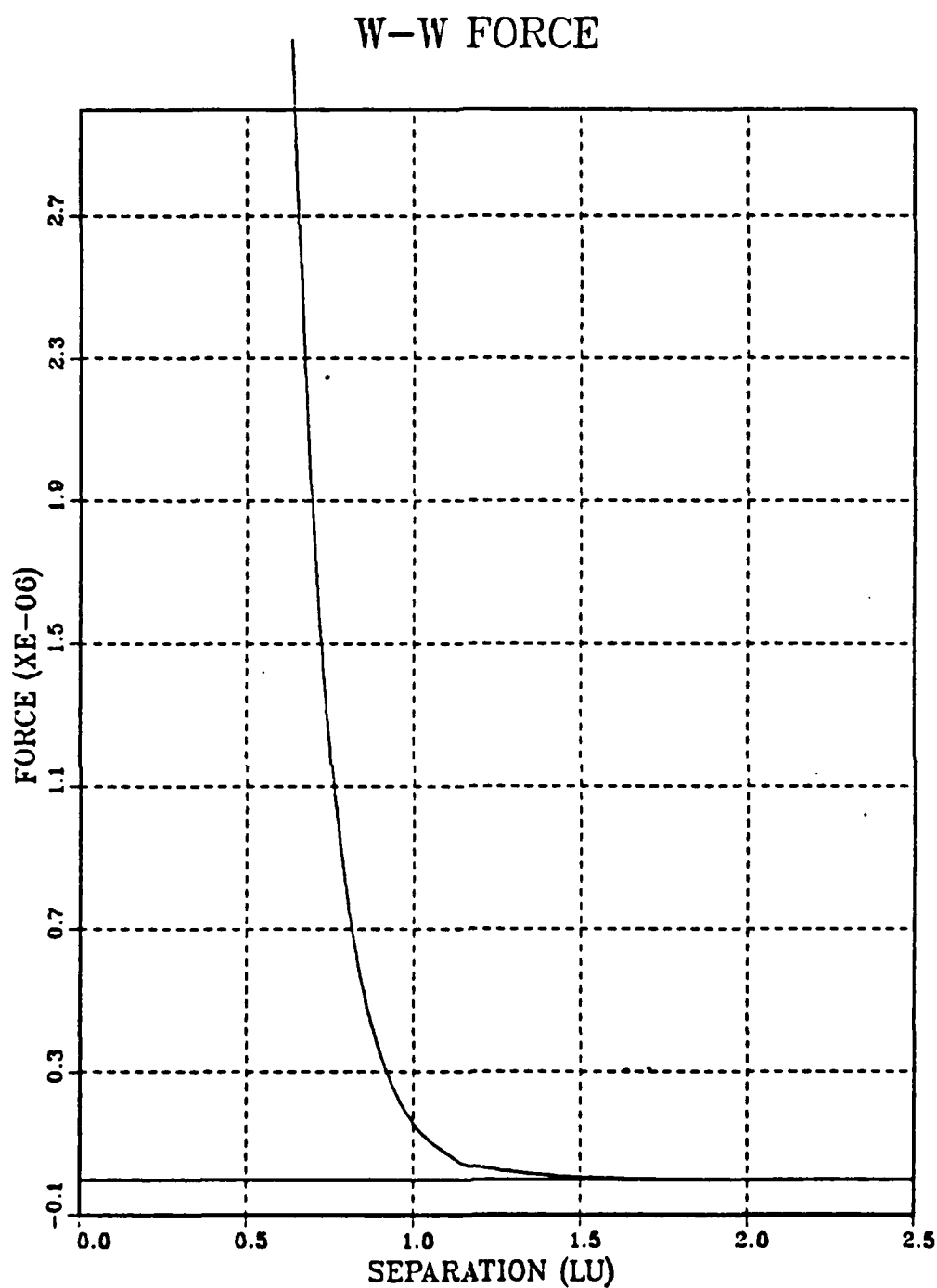
Fig. 14. Tungsten-Tungsten force function

53
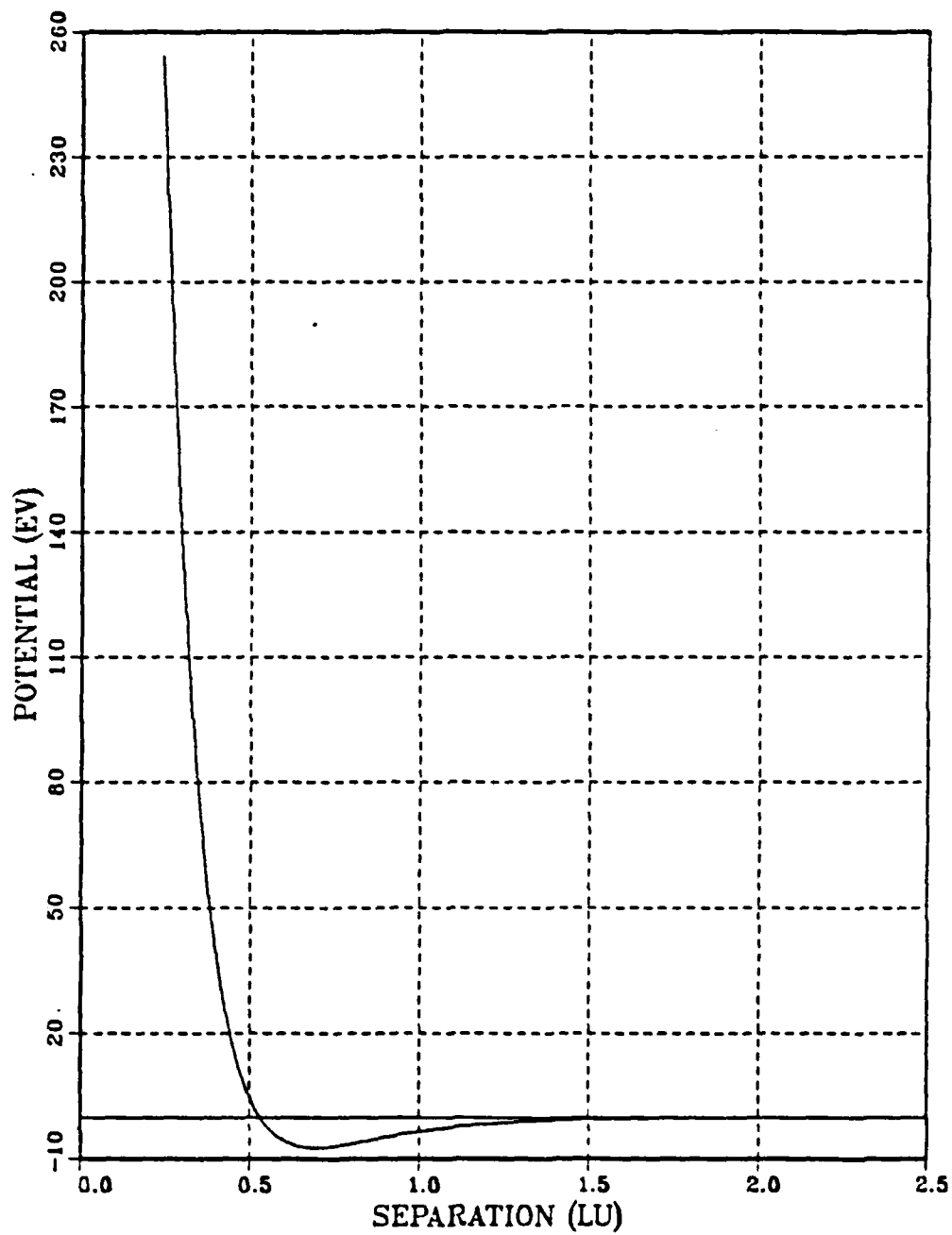
N–N POTENTIAL

Fig. 15. Nitrogen-Nitrogen potential function
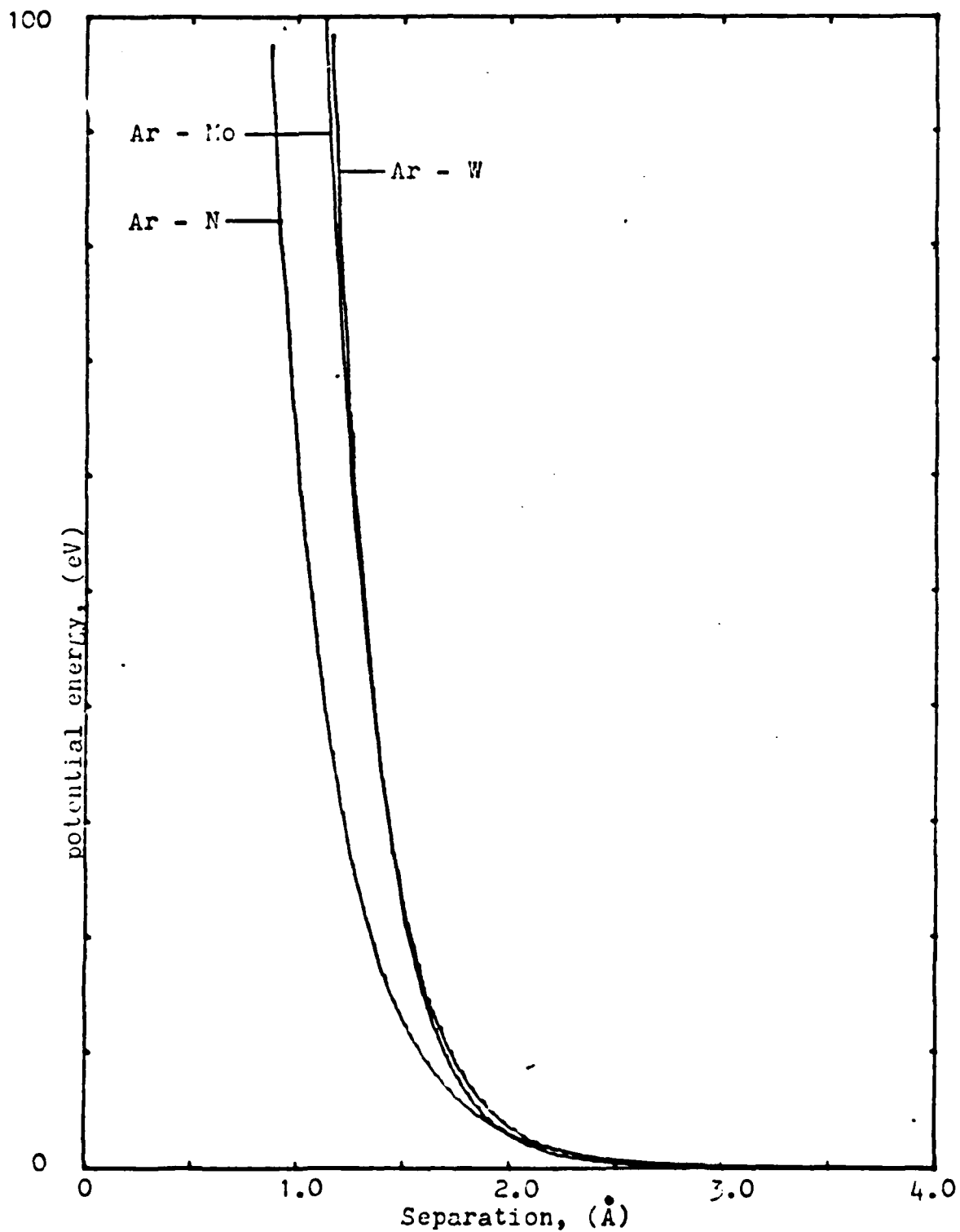
Fig. 16. Interatomic potential functions

55
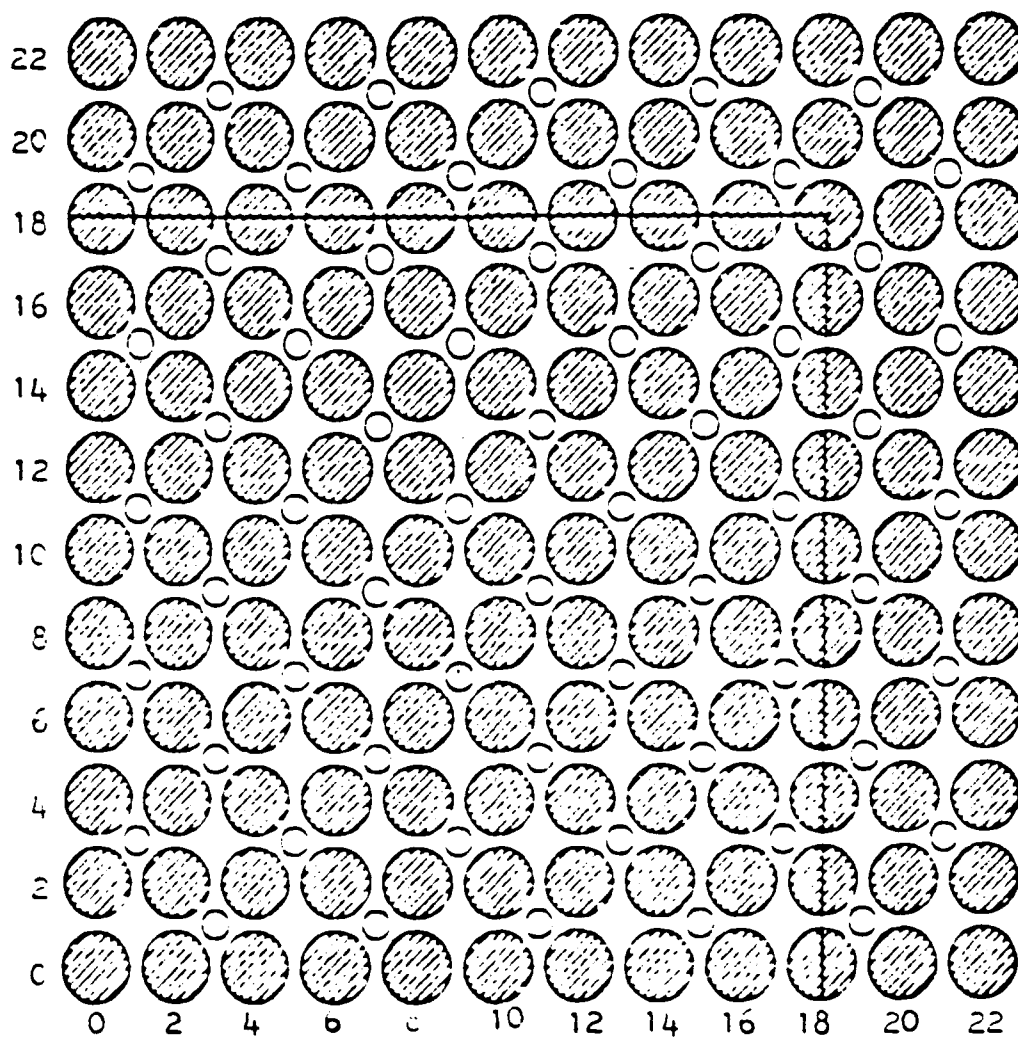
Small circles represent nitrogen atoms.
Numbers represent layers

Fig. 17. Top view of reacted target surface

56
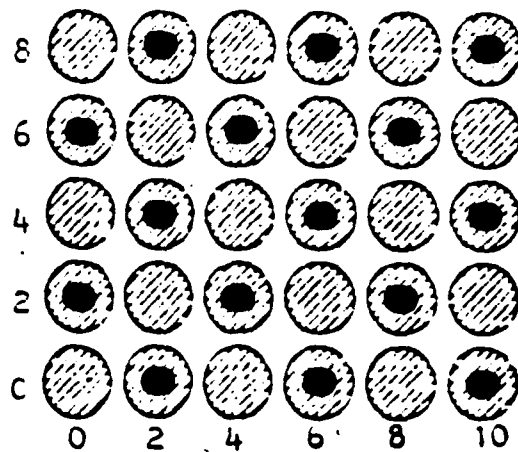
a) A-top position
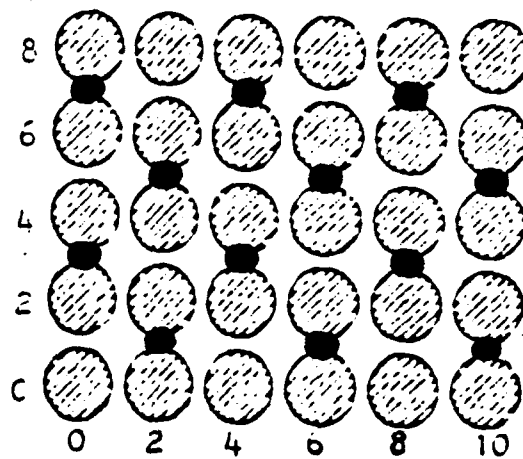
b) 2 fold position

Fig. 18. Nitrogen adatoms in various positions
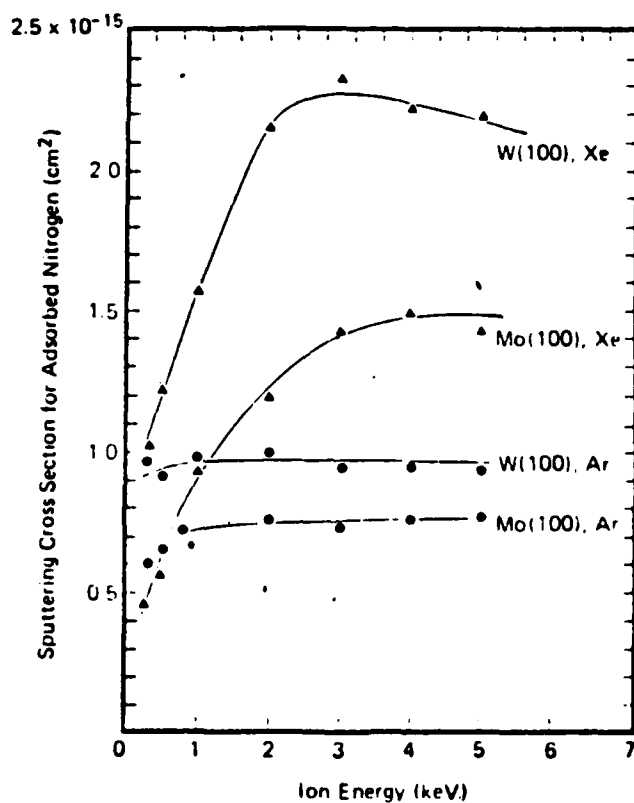
Fig. 19. Winters experimental sputtering ross section
results for adsorbed nitrogen

MO SPUTTERING CROSS SECTIONS
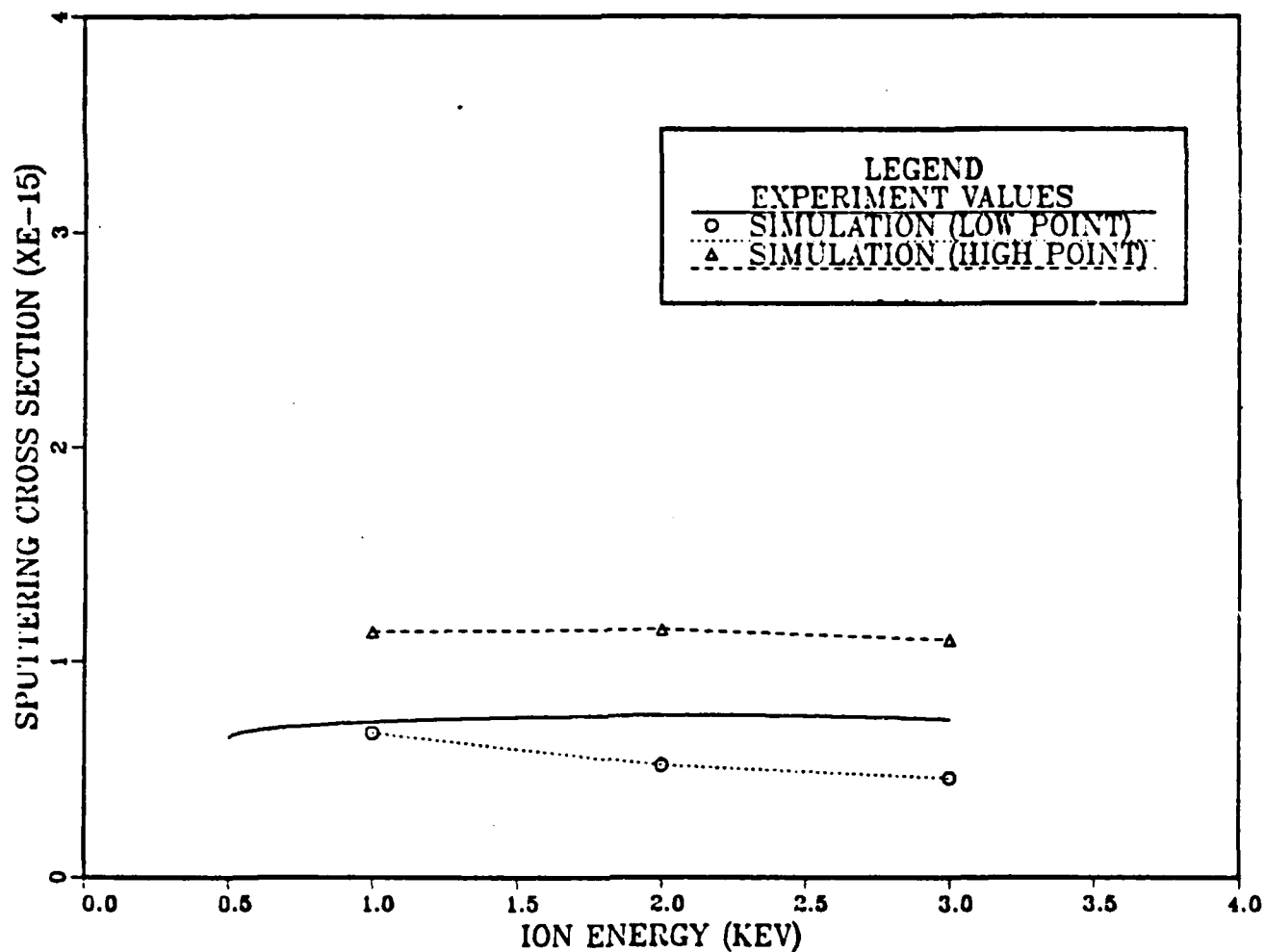
Fig. 20. Simulation nitrogen sputtering cross sections
for molybdenum target

59

W SPUTTERING CROSS SECTIONS
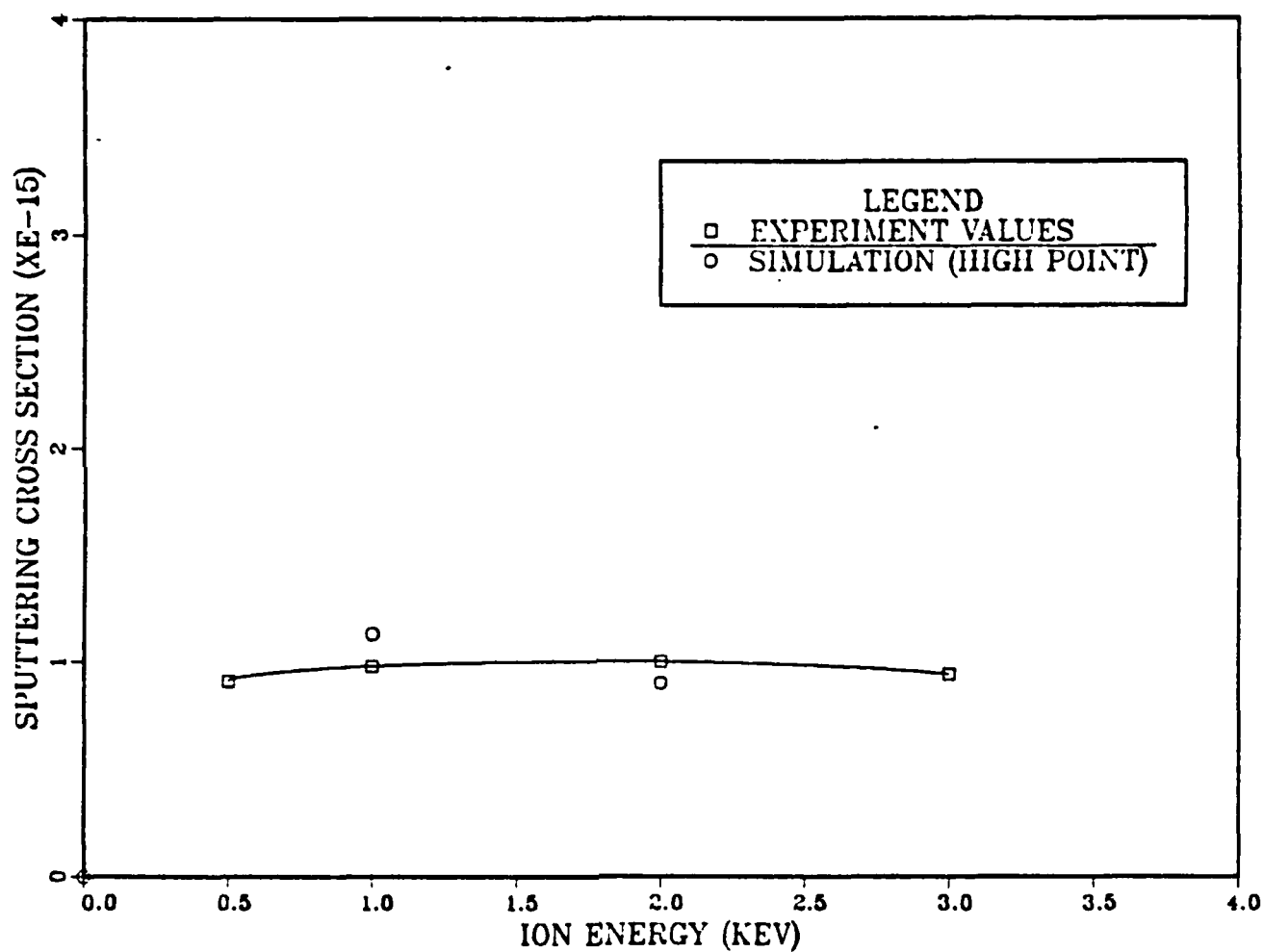
Fig. 21. Simulation nitrogen sputtering cross section
for tungsten target

2.000 W(001) +60N/A<001> COMBINED (N)(LOW)

EJECTED ATOM ENERGY DISTRIBUTION
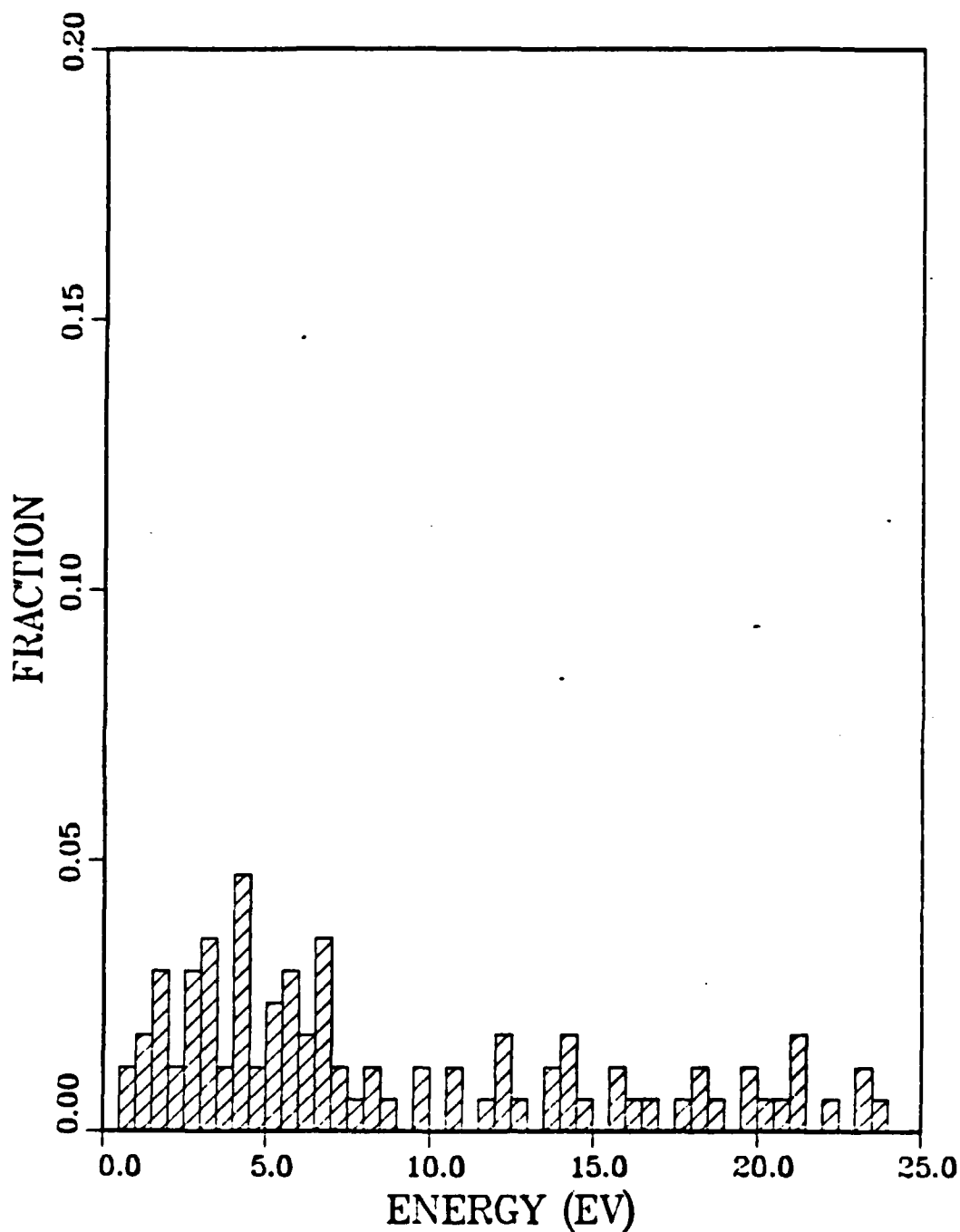
Fig. 22. Ejected nitrogen atom energy distribution from
a tungsten target assuming Argon energy of 2 keV
and adatom location of -.05 LU

2.000 MO(001) +60N/A<001> COMBINED (N)(LOW)

EJECTED ATOM ENERGY DISTRIBUTION
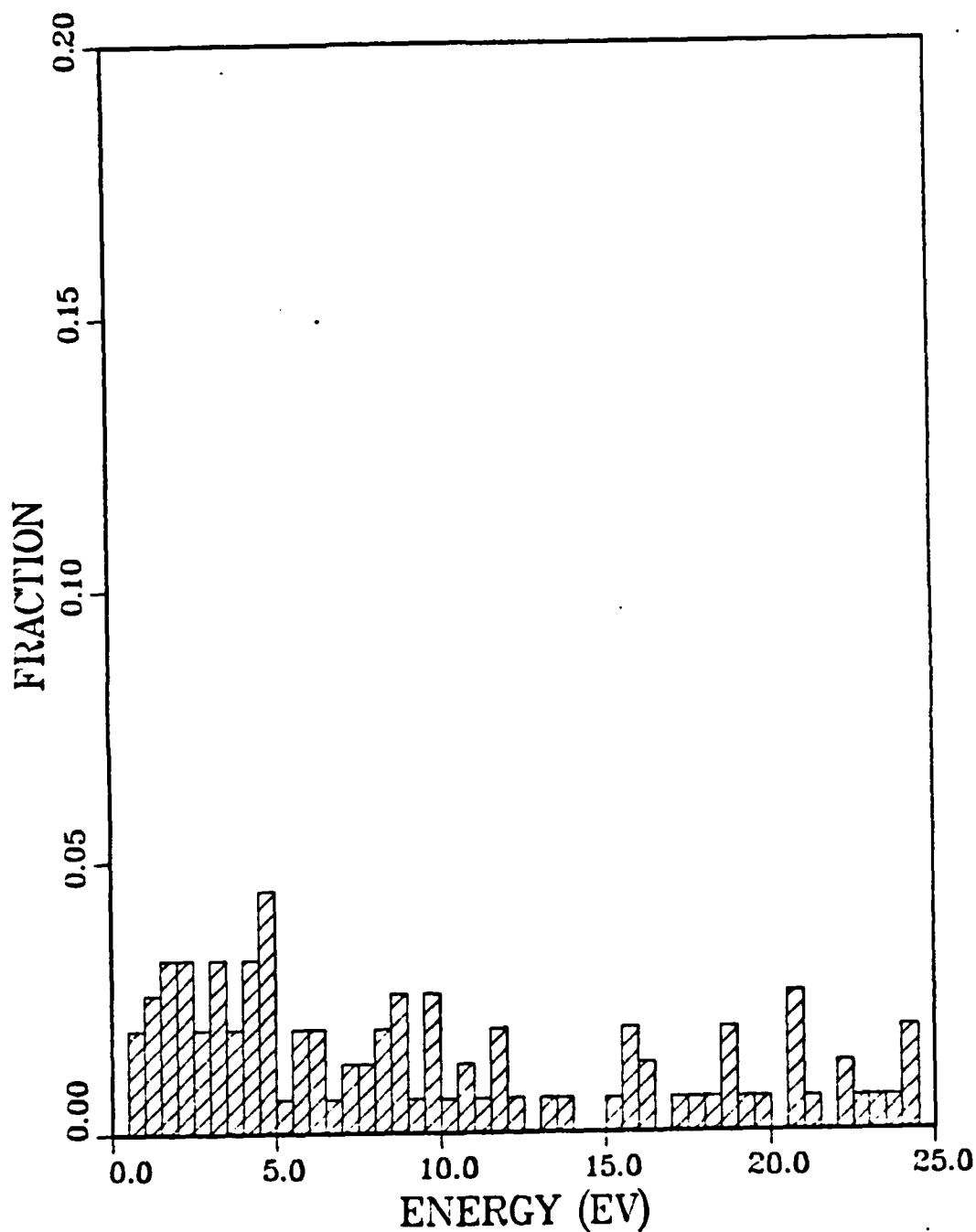
Fig. 23. Ejected Nitrogen energy distribution from a molybdenum target assuming argon energy 2 keV and adatom location -.05 LU

62

2.000 MO(001) +60N/A<001> COMBINED(N)(HIGH)

EJECTED ATOM ENERGY DISTRIBUTION
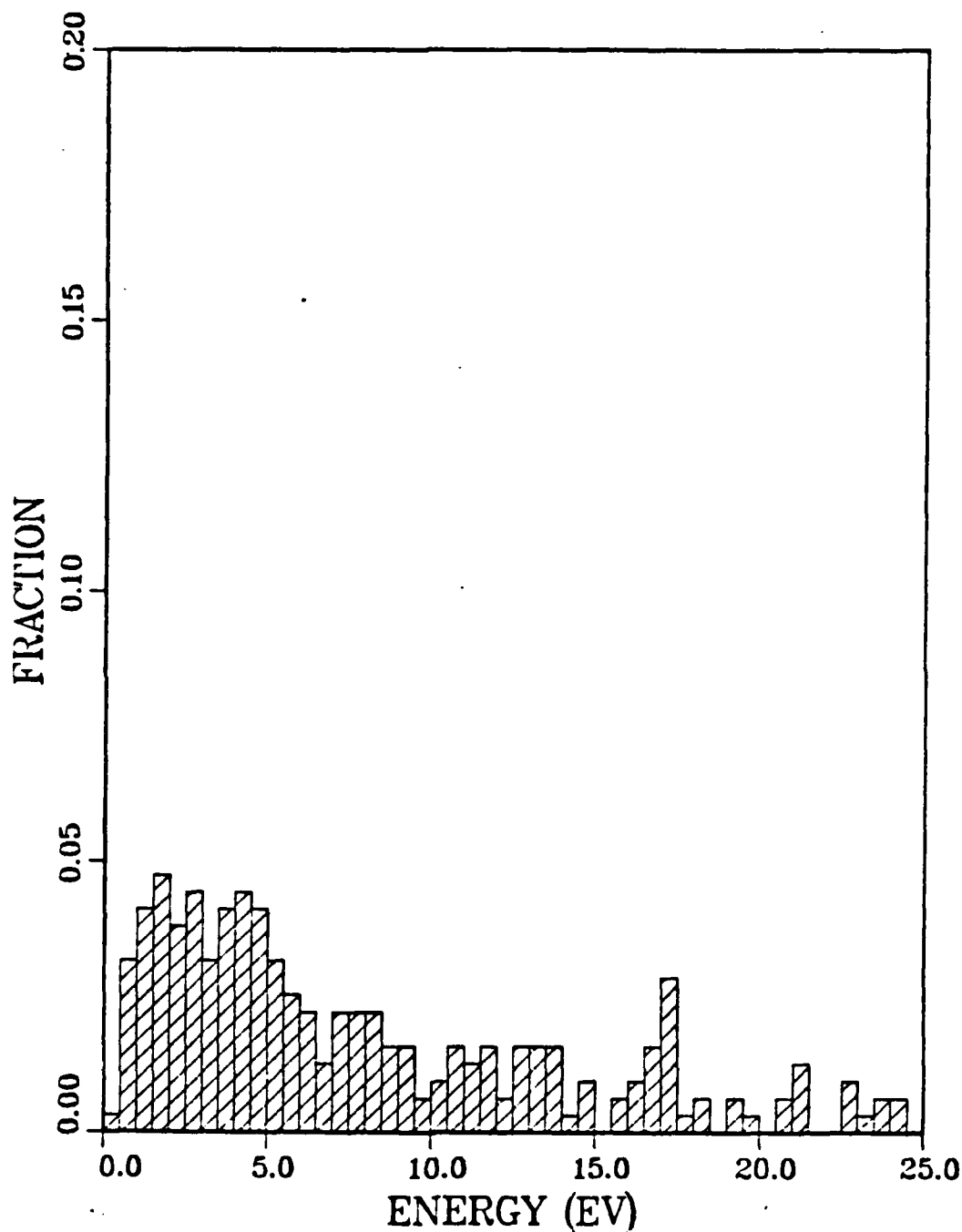
Fig. 24. Ejected nitrogen energy distribution from molybdenum target assuming argon energy of 2 keV and adatom position .387 LU

63

2.000 W(001) +60N/A<001> COMBINED(N)(HIGH)

EJECTED ATOM ENERGY DISTRIBUTION
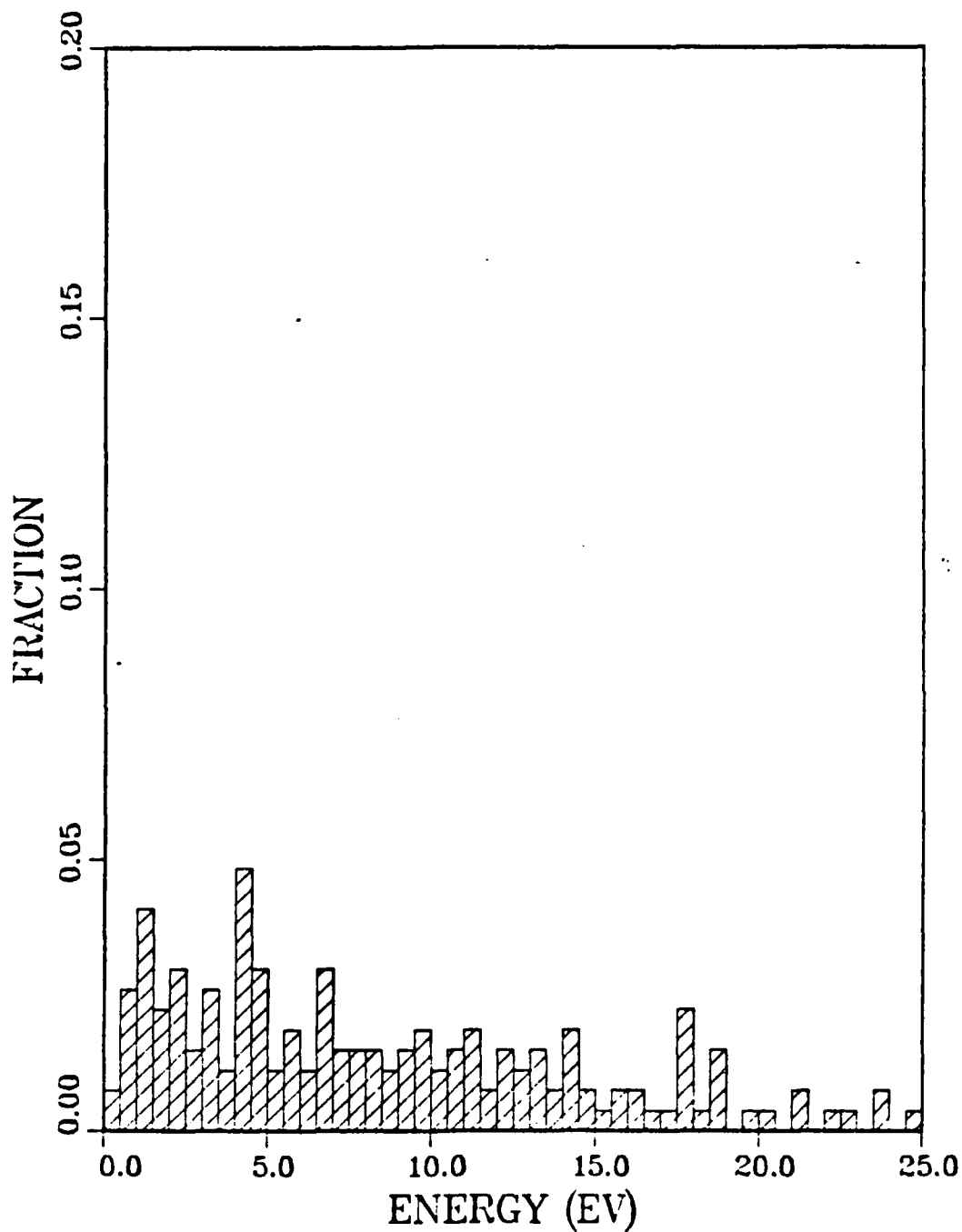
Fig. 25. Ejected nitrogen atom energy distribution from a
simulated tungsten target assuming argon energy
of 2 keV and adatom position .487 LU

64

2.000 MO(001) +60N/A<001> NITROGEN (NH)(HIGH)

SPOT PATTERN
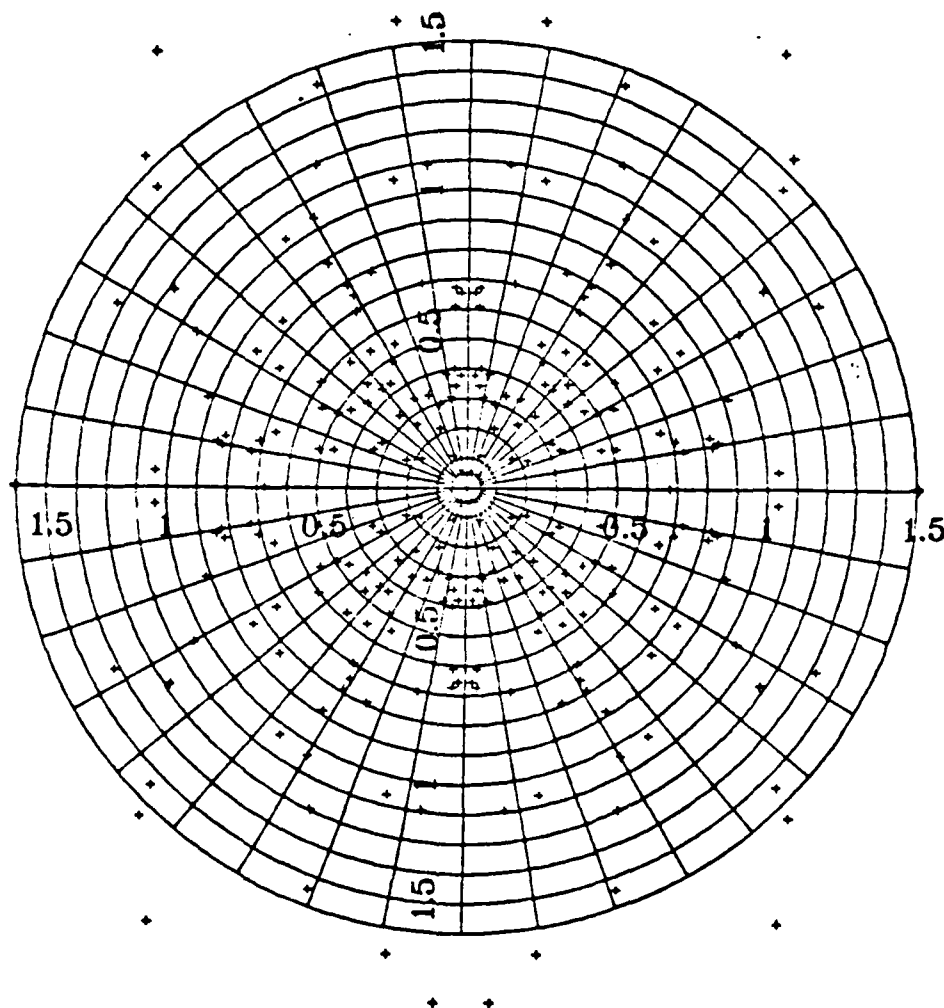
Fig. 26. Simulation ejected nitrogen spot pattern from a
molybdenum target assuming argon energy of 2 keV
and adatom location .387 LU

65

2.000 W(001) +60N/A<001> (23X8X23) TUNGSTEN (NH)
ATOM YIELD PER IMPACT POINT
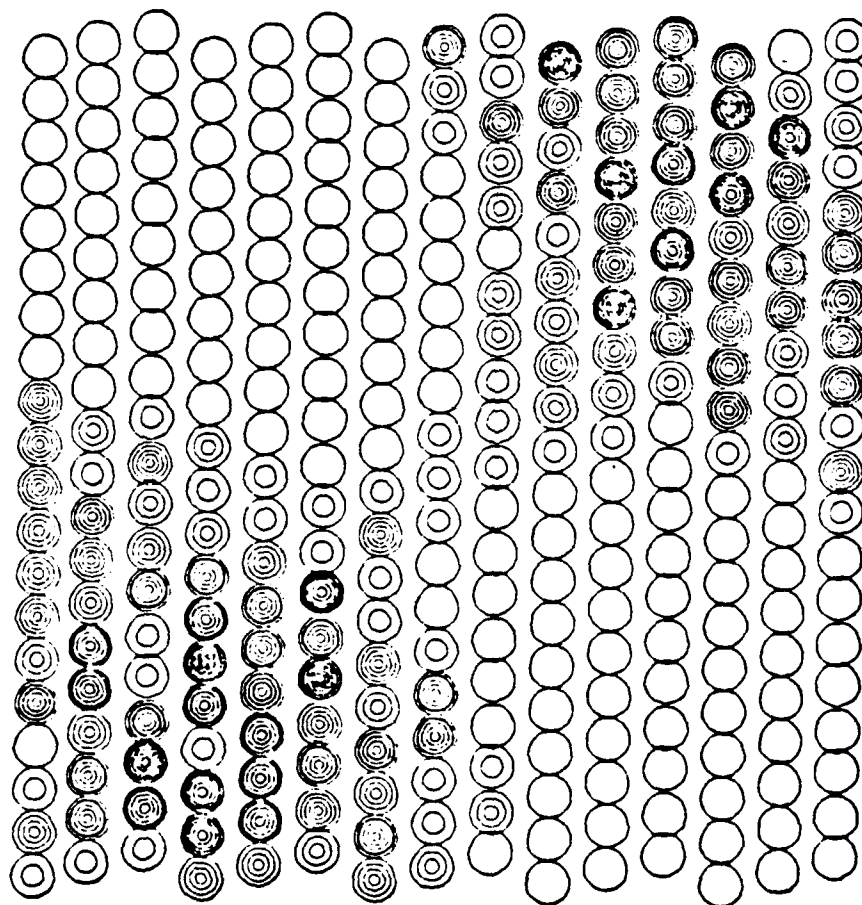
Fig. 27. Simulation atom yield per impact point for a
tungsten target bombarded with 2 keV argon

2.000 MO(001) +60N/A<001> MOLYBDENUM (NH)(HIGH)

ATOM YIELD PER IMPACT POINT
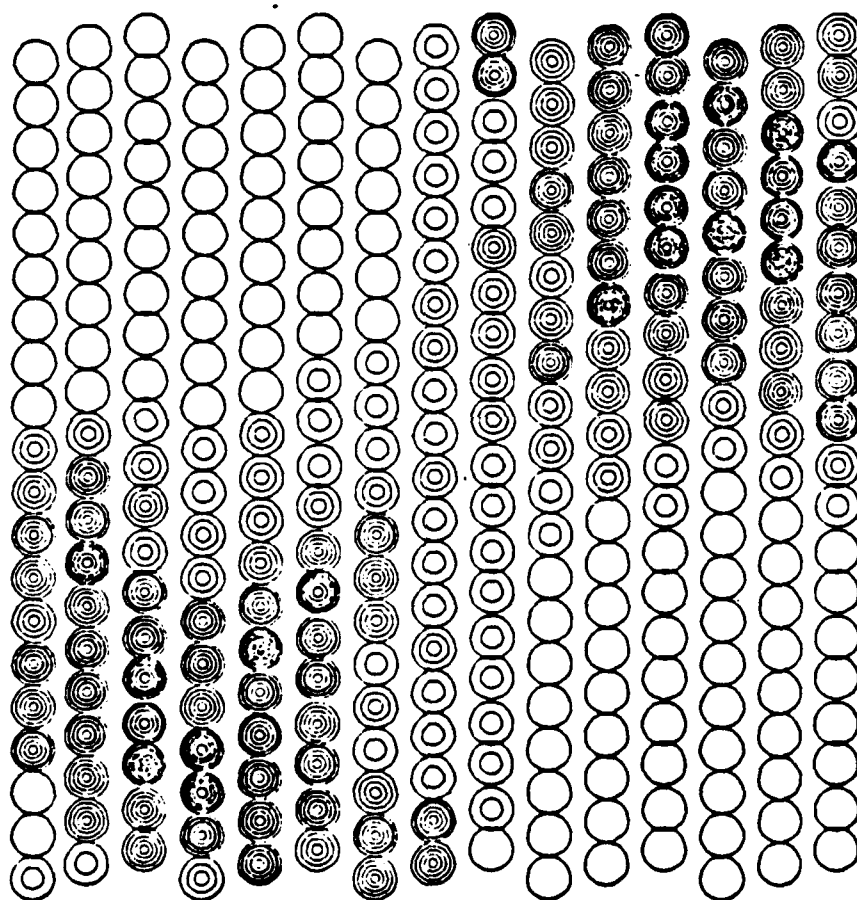
Fig. 28. Simulation atom yield per impact point from a
molybdenum target assuming 2 keV argon ion

2.000 MO(001) +60N/A<001> MOLYBDENUM (NH)(HIGH)
ATOM EJECTION PROBABILITY
BCC (001)
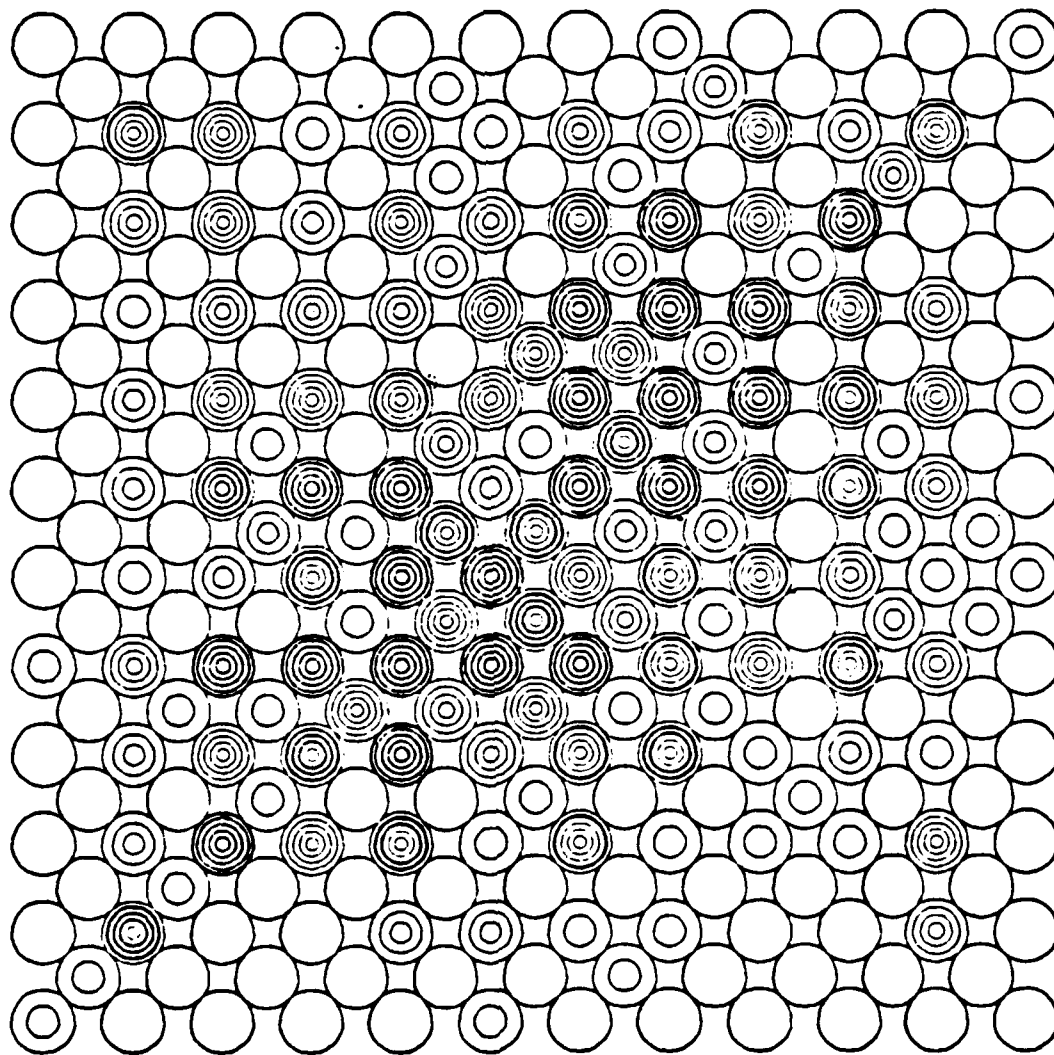
Fig. 29. Simulation atom ejection probability from a
BCC (001) molybdenum target assuming a 2keV
argon ion

2.000 W(001) +60N/A<001> (23X8X23) TUNGSTEN (NH)
ATOM EJECTION PROBABILITY
BCC (001)
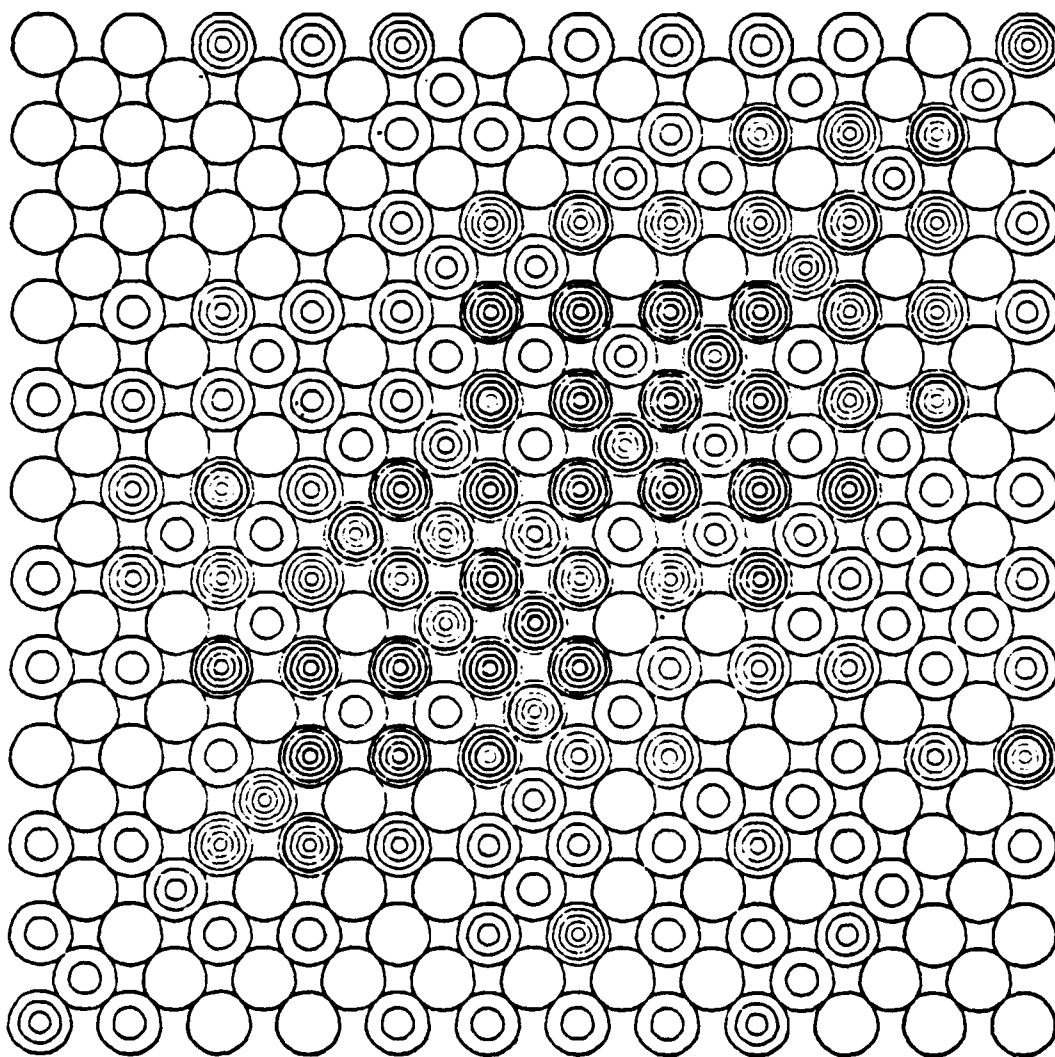
Fig. 30. Simulation atom ejection probability from a
BCC (001) tungsten target assuming an argon
ion energy of 2 keV

1.000 MO(001) +60N/A<001> MOLYBDENUM (NH)(LOW)

SPOT PATTERN
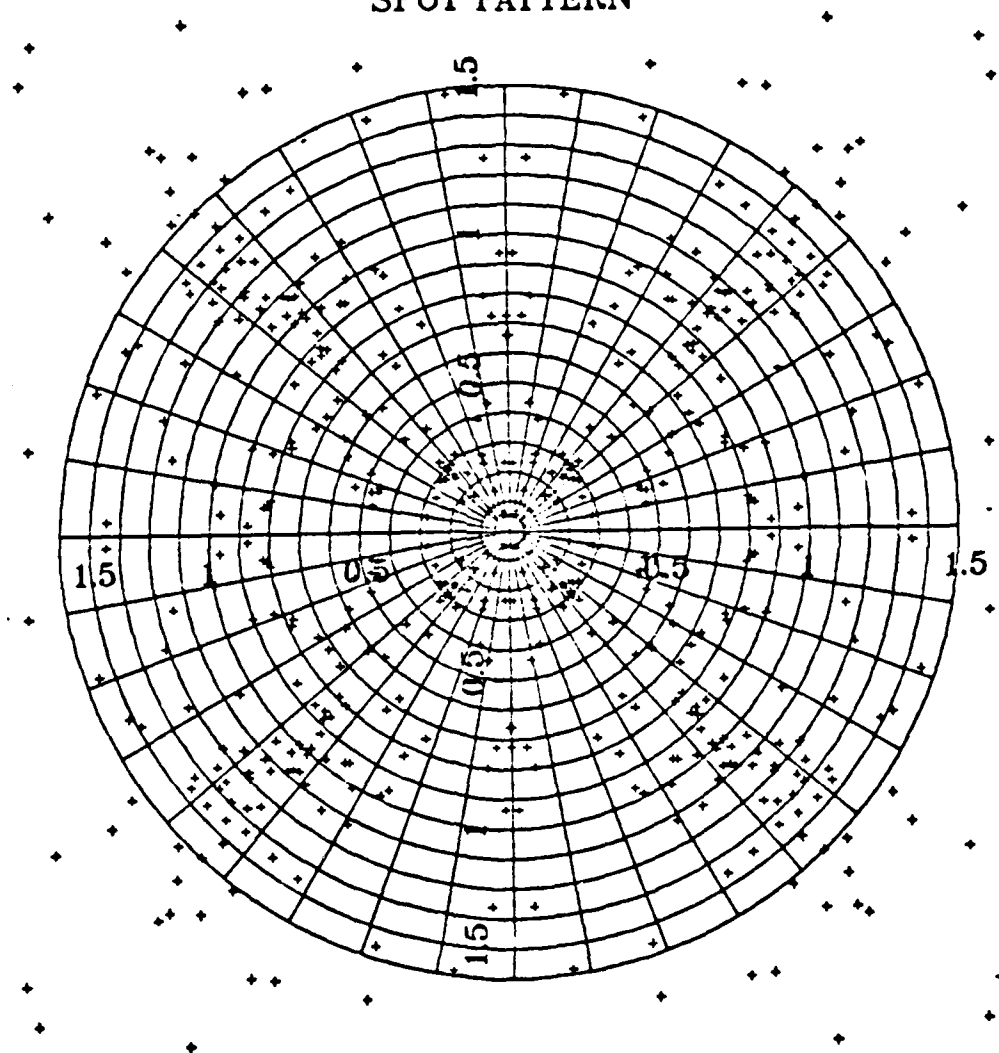
Fig. 31. Simulation molybdenum ejection spot pattern
assuming a 1 keV argon ion

2.000 W(001) +60N/A<001> TUNGSTEN (NH)(LOW)

SPOT PATTERN
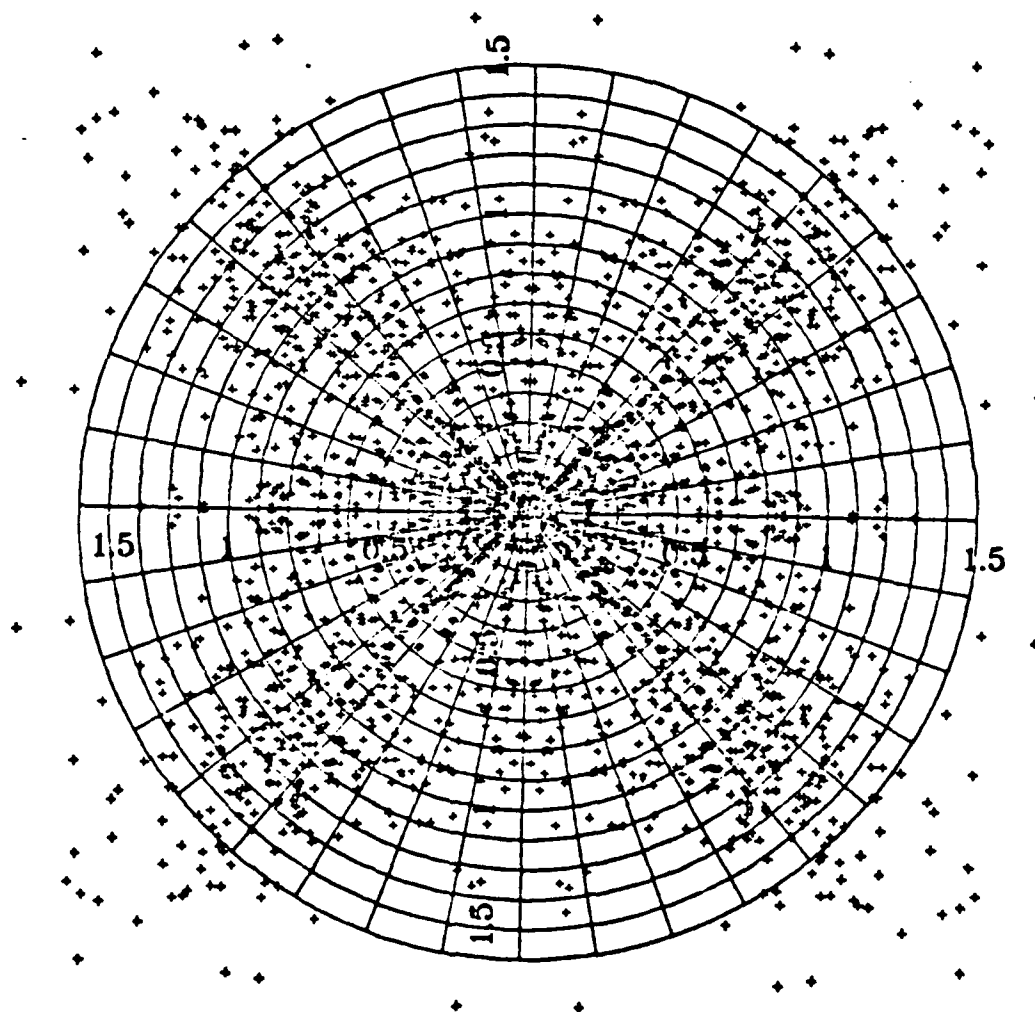
Fig. 32. Simulation tungsten ejection spot pattern assuming 2 keV argon ion

71

3.000 MO(001) +60N/A<001> COMBINED(MO)(HIGH)

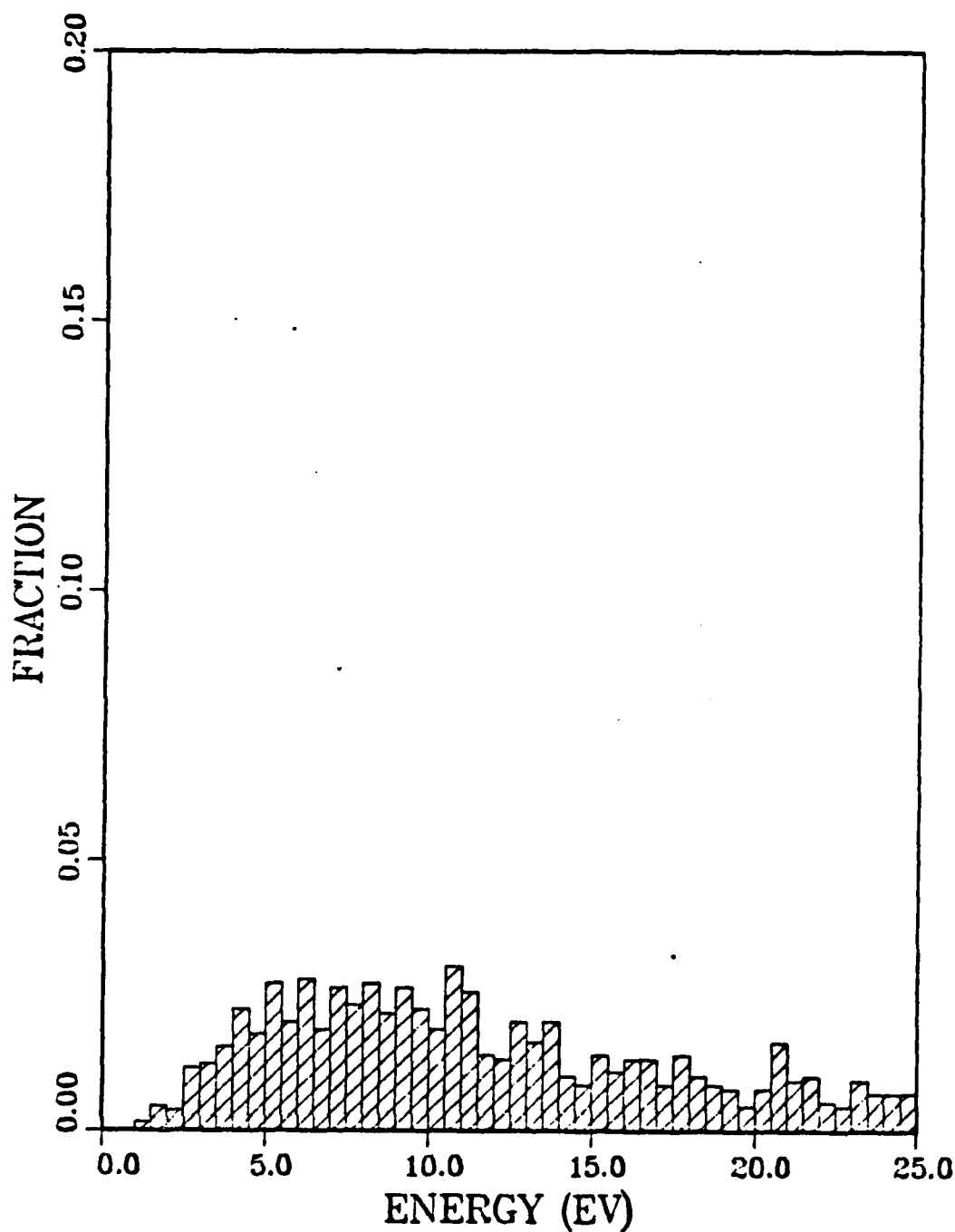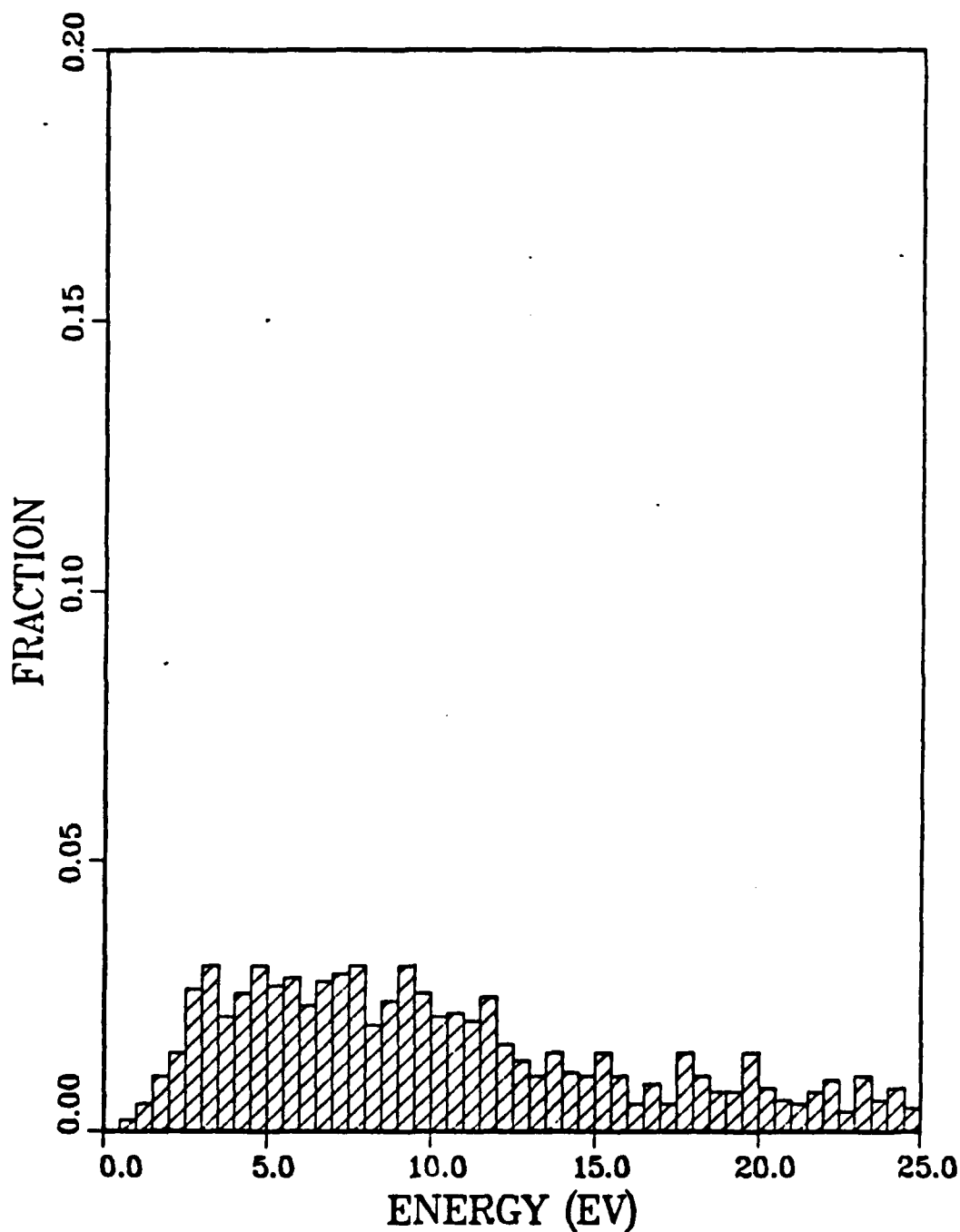### EJECTED ATOM ENERGY DISTRIBUTION

Fig. 33. Simulated ejected atom energy distribution from molybdenum target with nitrogen adatoms assuming a 3 keV argon ion

2.000 W(001) +60N/A<001> COMBINED(W)(HIGH)

EJECTED ATOM ENERGY DISTRIBUTION
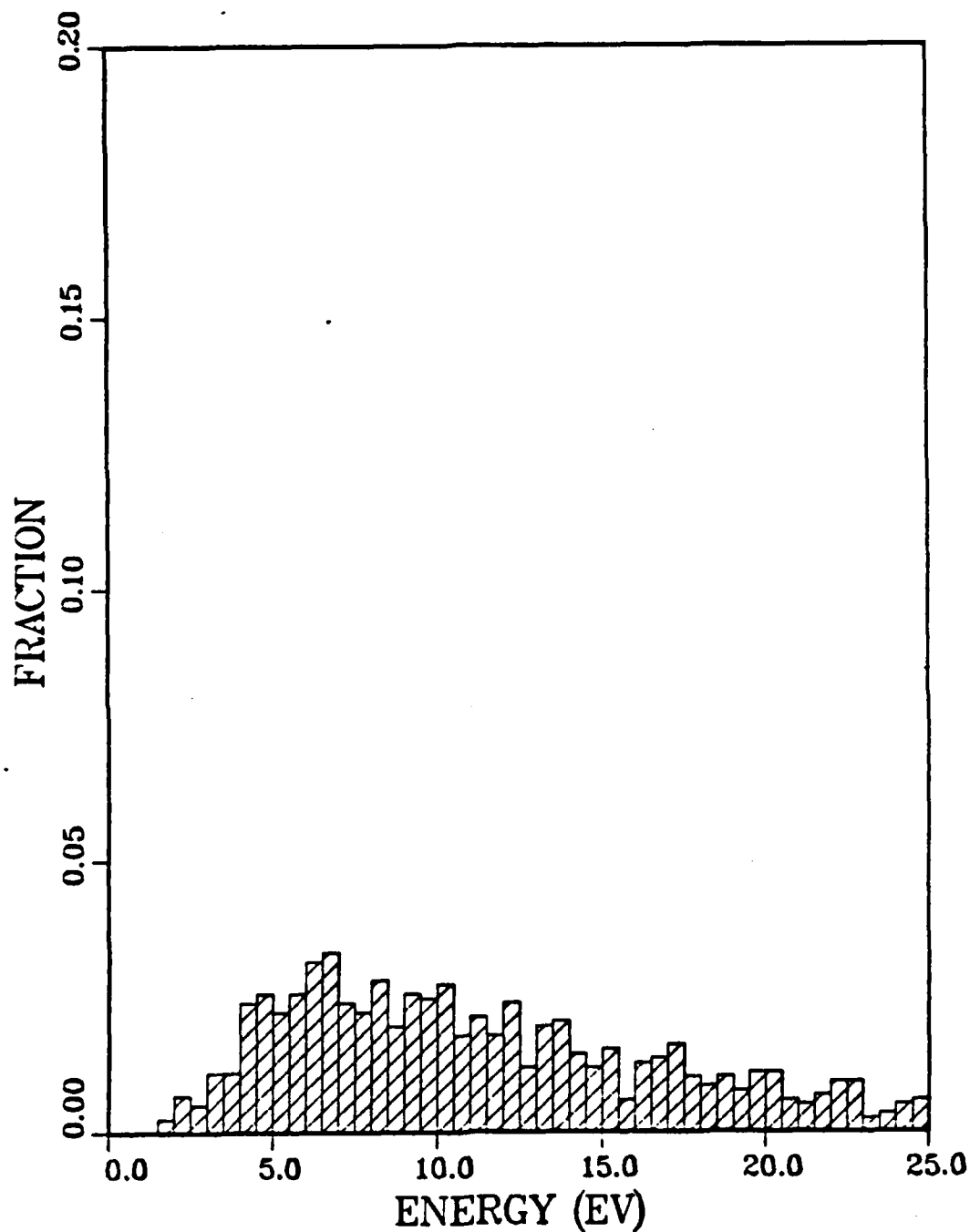
Fig. 34. Simulated ejected atom energy distribution from
tungsten target with nitrogen adatoms assuming
a 2 keV argon ion

1.000 W(001) +60N/A<001> COMBINED(W)(HIGH)

EJECTED ATOM ENERGY DISTRIBUTION

Fig. 35. Simulation ejected atom energy distribution from tungsten target with nitrogen adatoms assuming a 1 keV argon ion

74

2.000 MO(001) +60N/A<001> COMBINED(MO)(LOW)

EJECTED ATOM ENERGY DISTRIBUTION

Fig. 36. Simulation ejected atom energy distribution from molybdenum target with nitrogen adatoms assuming a 2 keV argon ion

2.000 MO(001) CLEAN (23X8X23) MOLYBDENUM
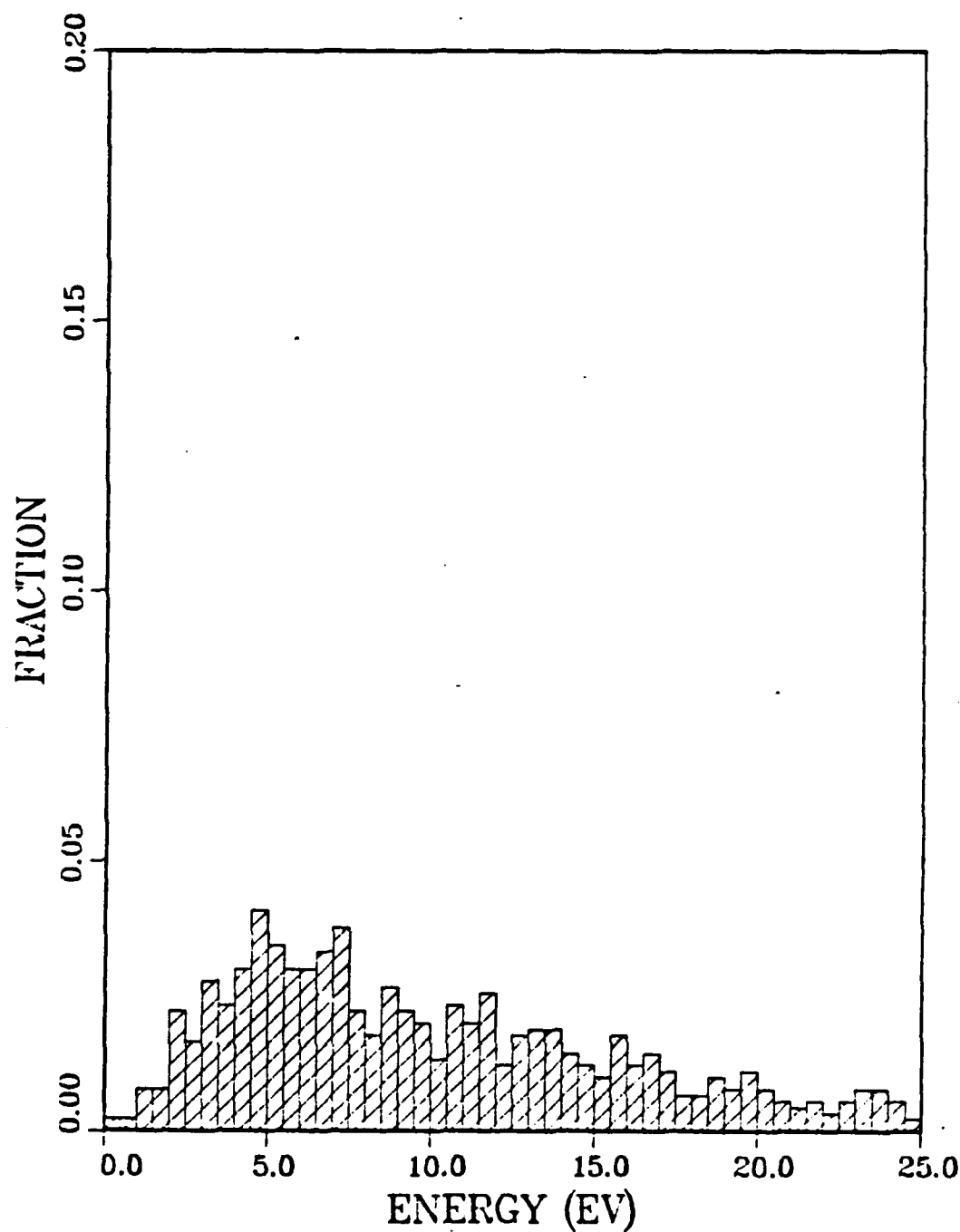
EJECTED ATOM ENERGY DISTRIBUTION

Fig. 37. Simulated ejected atom energy distribution from clean molybdenum target assuming a 2 keV argon ion

2.000 W(001) CLEAN (23X8X23) TUNGSTEN
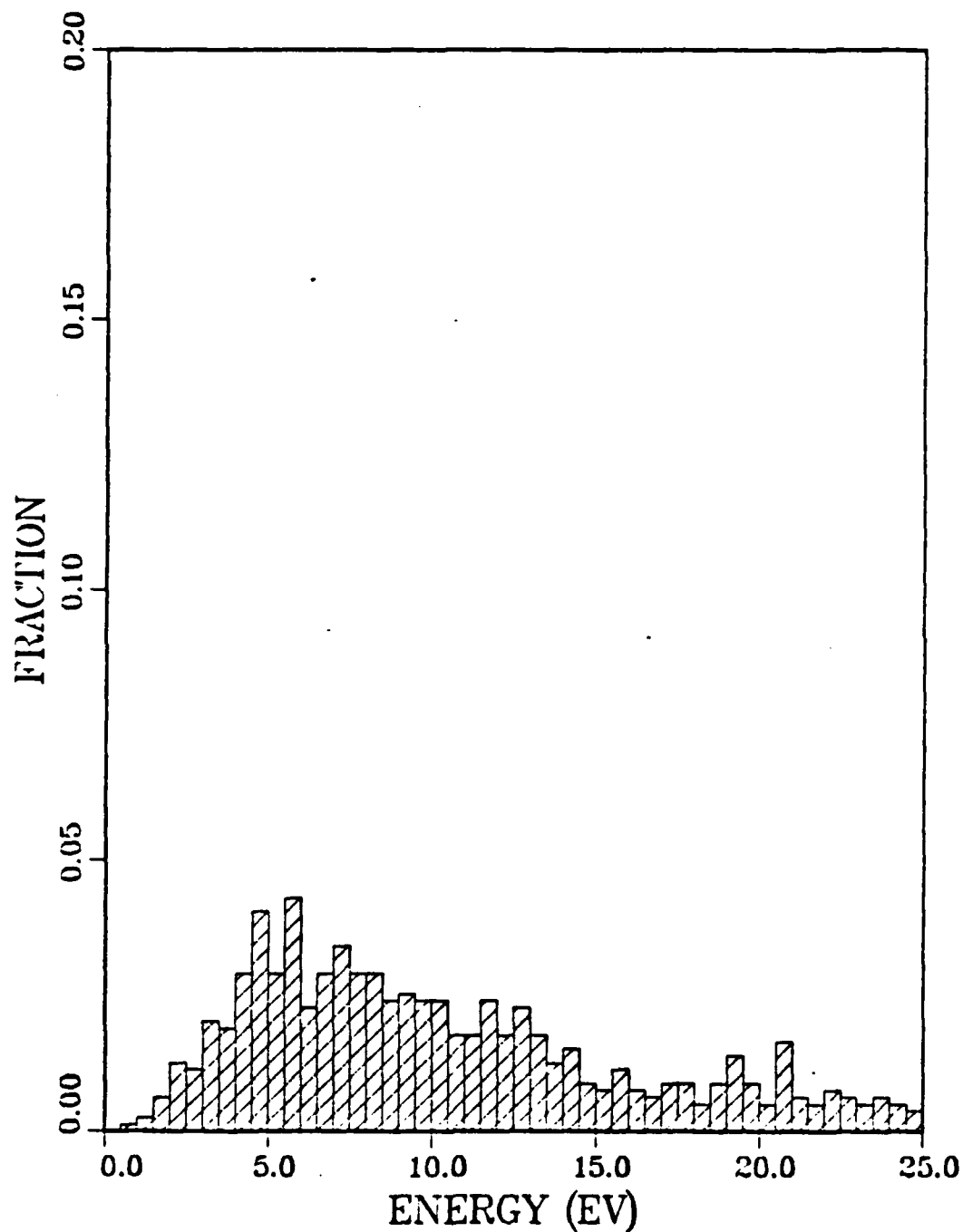
EJECTED ATOM ENERGY DISTRIBUTION

Fig. 38. Simulated ejected atom energy distribution from
clean tungsten target assuming a 2 keV argon ion

3.000 MO(001) +60N/A<001> COMBINED(MO)(HIGH)
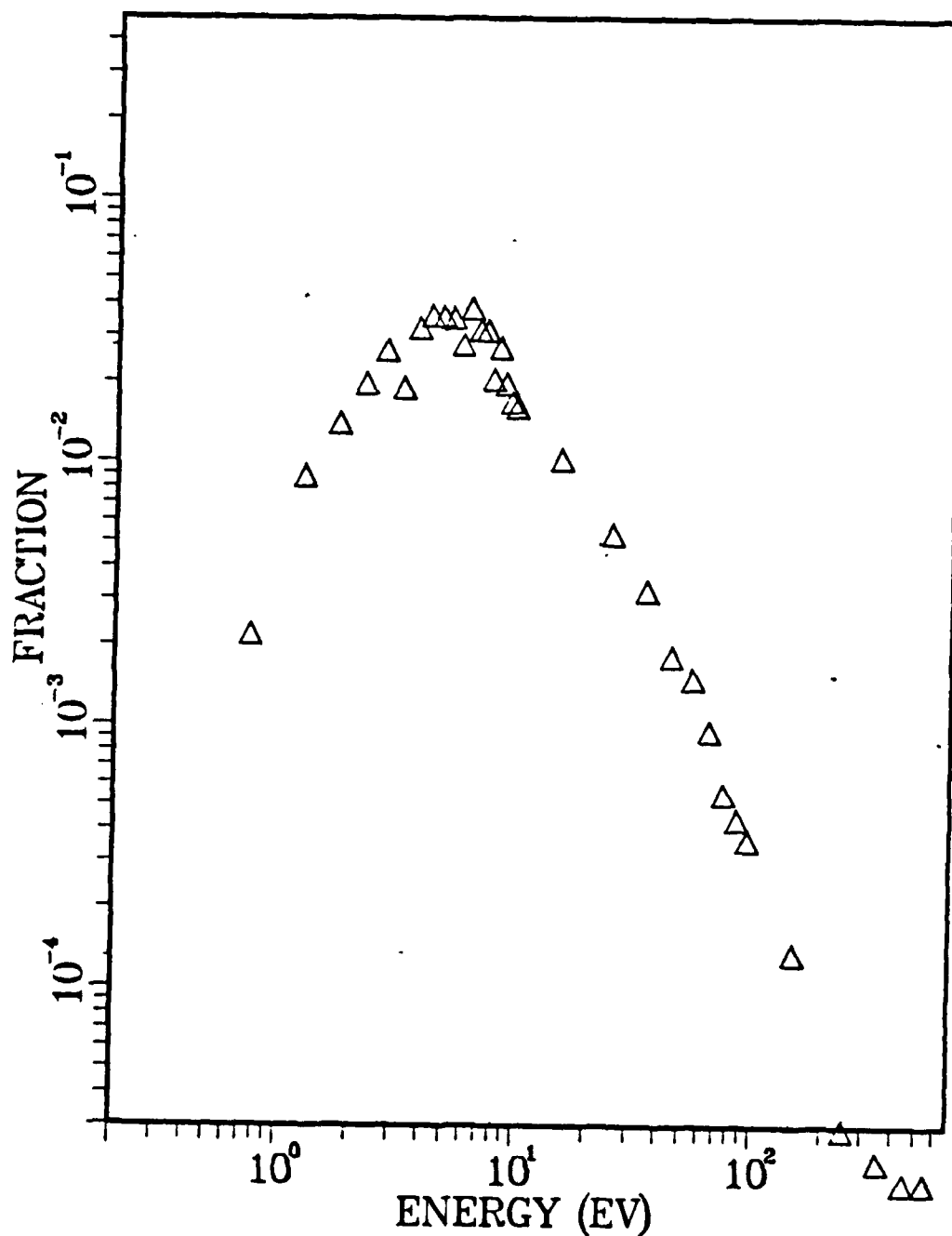
EJECTED ATOM ENERGY DISTRIBUTION

Fig. 39. Log-Log ejected atom energy distribution from a molybdenum target with nitrogen adatoms assuming 3 keV argon ion

1.000 W(001) +60N/A<001> COMBINED(W)(HIGH)

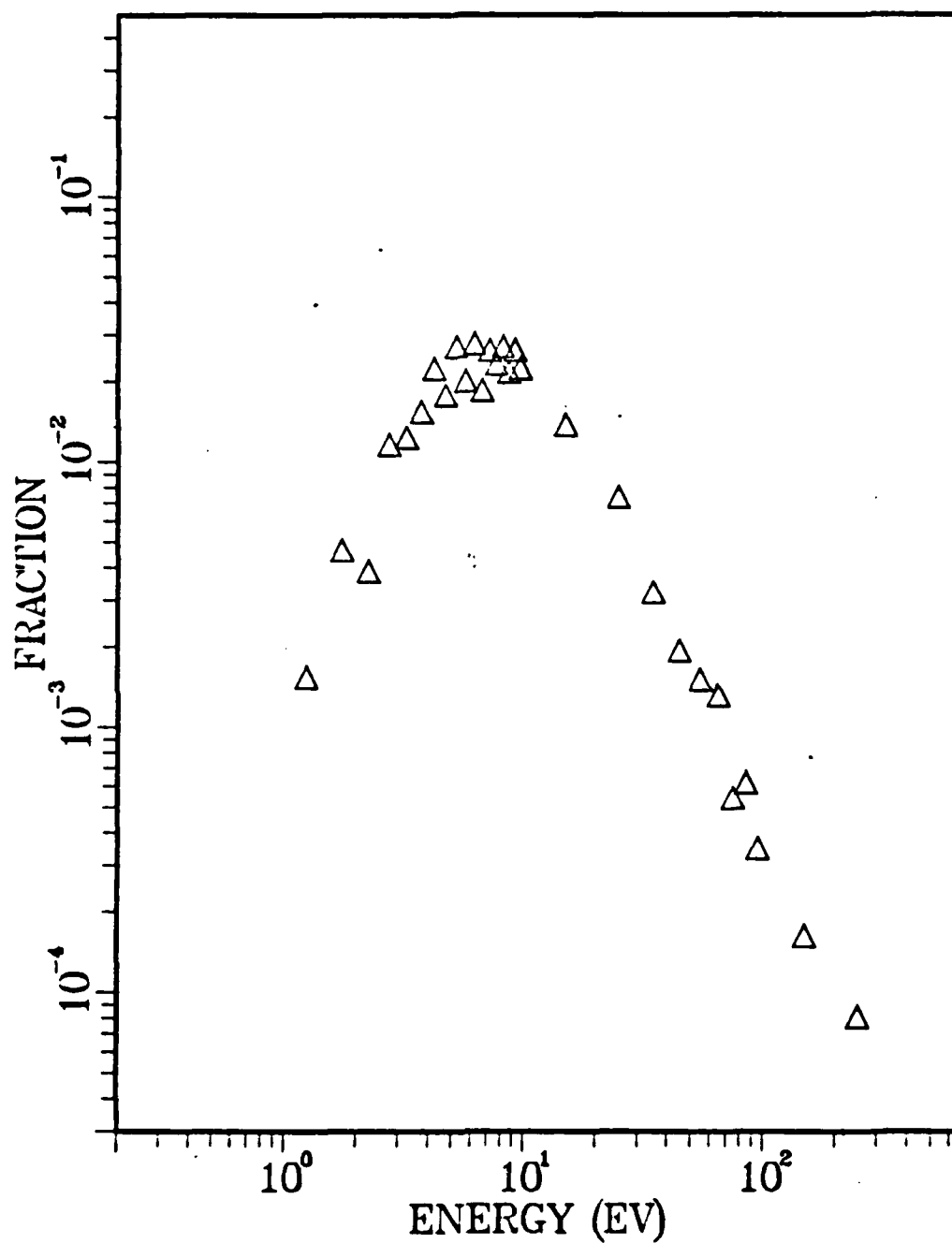## EJECTED ATOM ENERGY DISTRIBUTION

Fig. 40. Log-Log ejected atom energy distribution from tungsten target with nitrogen adatoms assuming 1 keV argon ion

2.000 W(001) +60N/A<001> COMBINED(W)(HIGH)

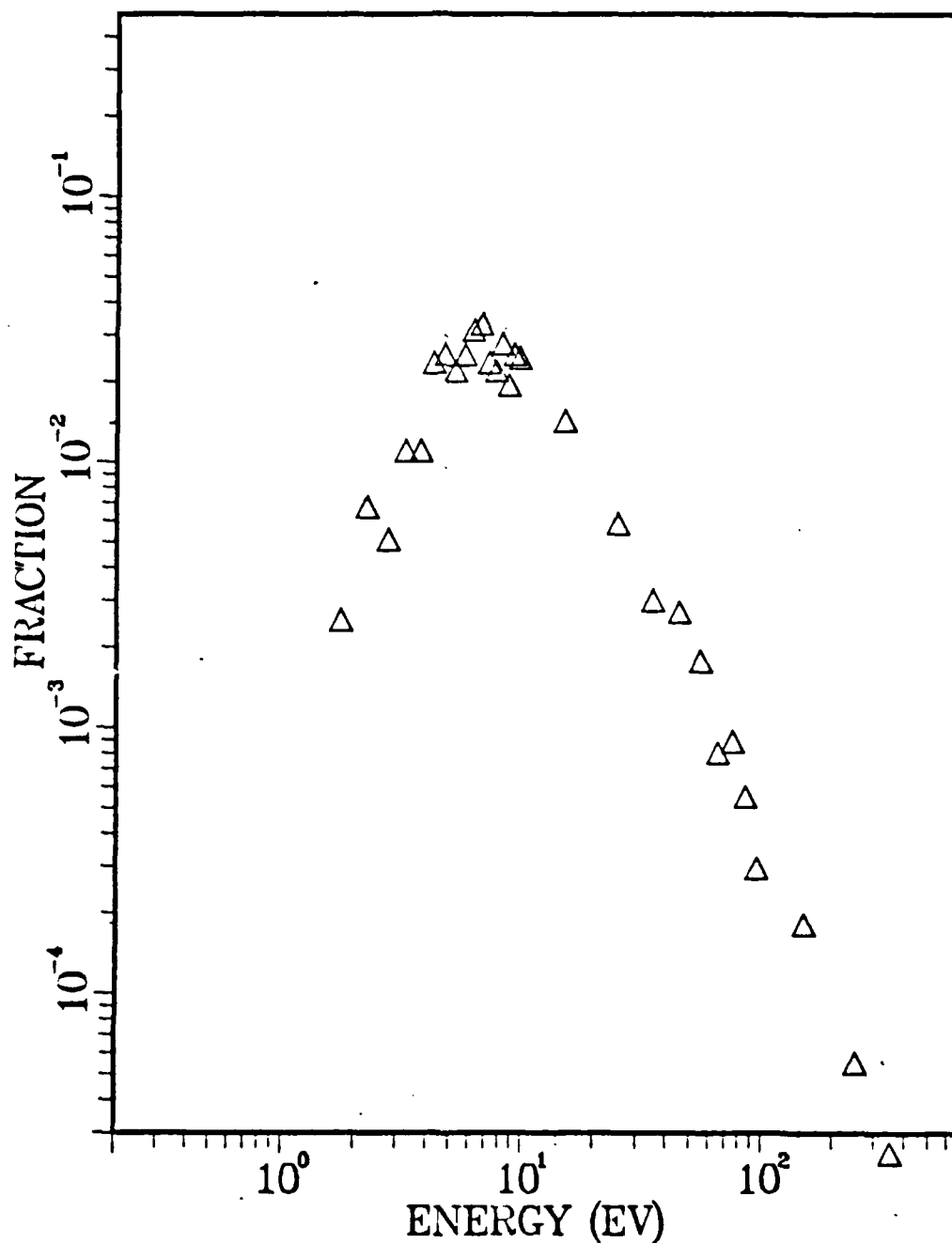### EJECTED ATOM ENERGY DISTRIBUTION

Fig. 41. Log-Log ejected atom energy distribution from tungsten target with nitrogen adatoms assuming 2 keV argon ion

2.000 W(001) CLEAN (23X8X23) TUNGSTEN
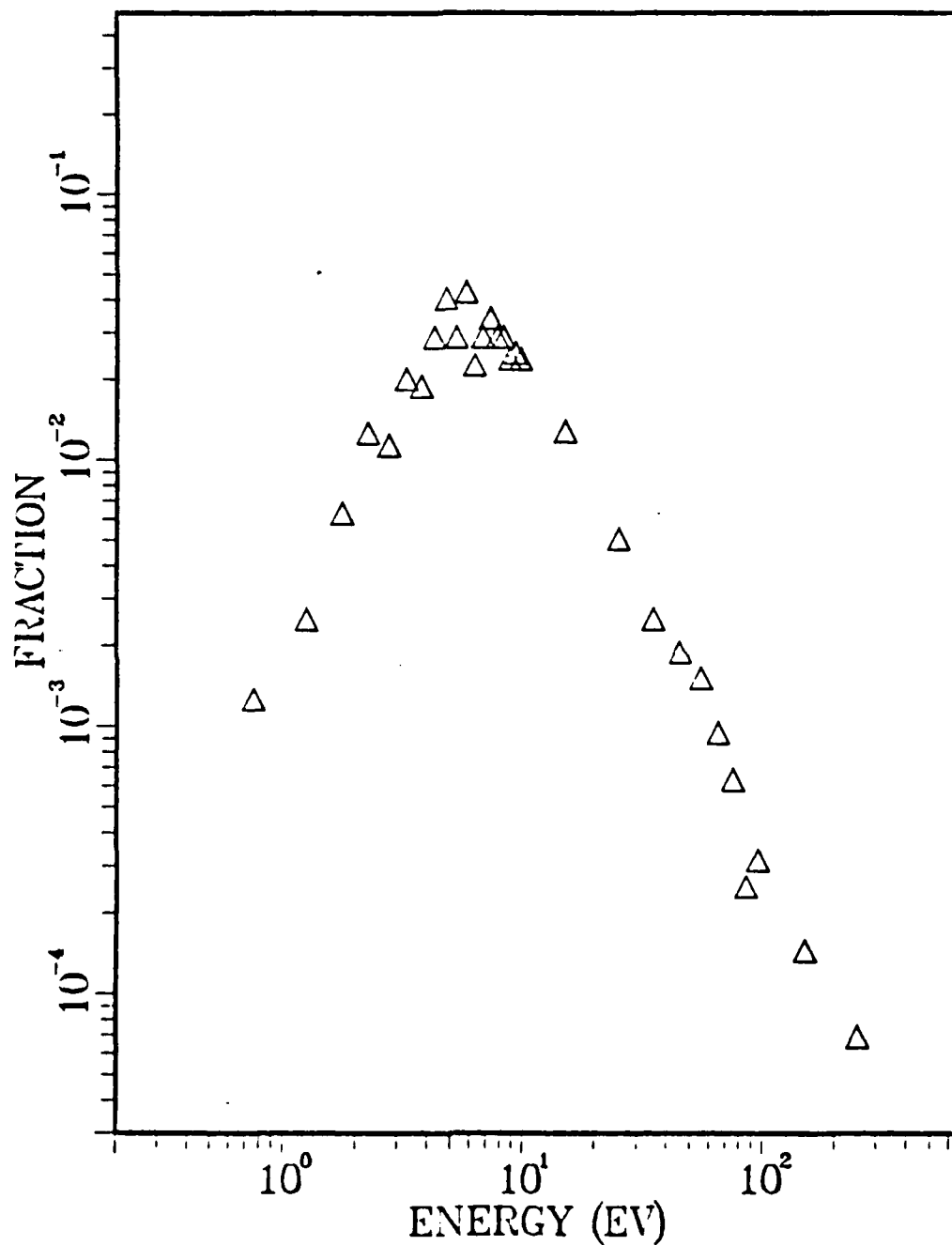### EJECTED ATOM ENERGY DISTRIBUTION

Fig. 42. Log-Log ejected atom energy distribution from clean tungsten assuming 2keV argon ion

2.000 MO(001) CLEAN (23X8X23) MOLYBDENUM
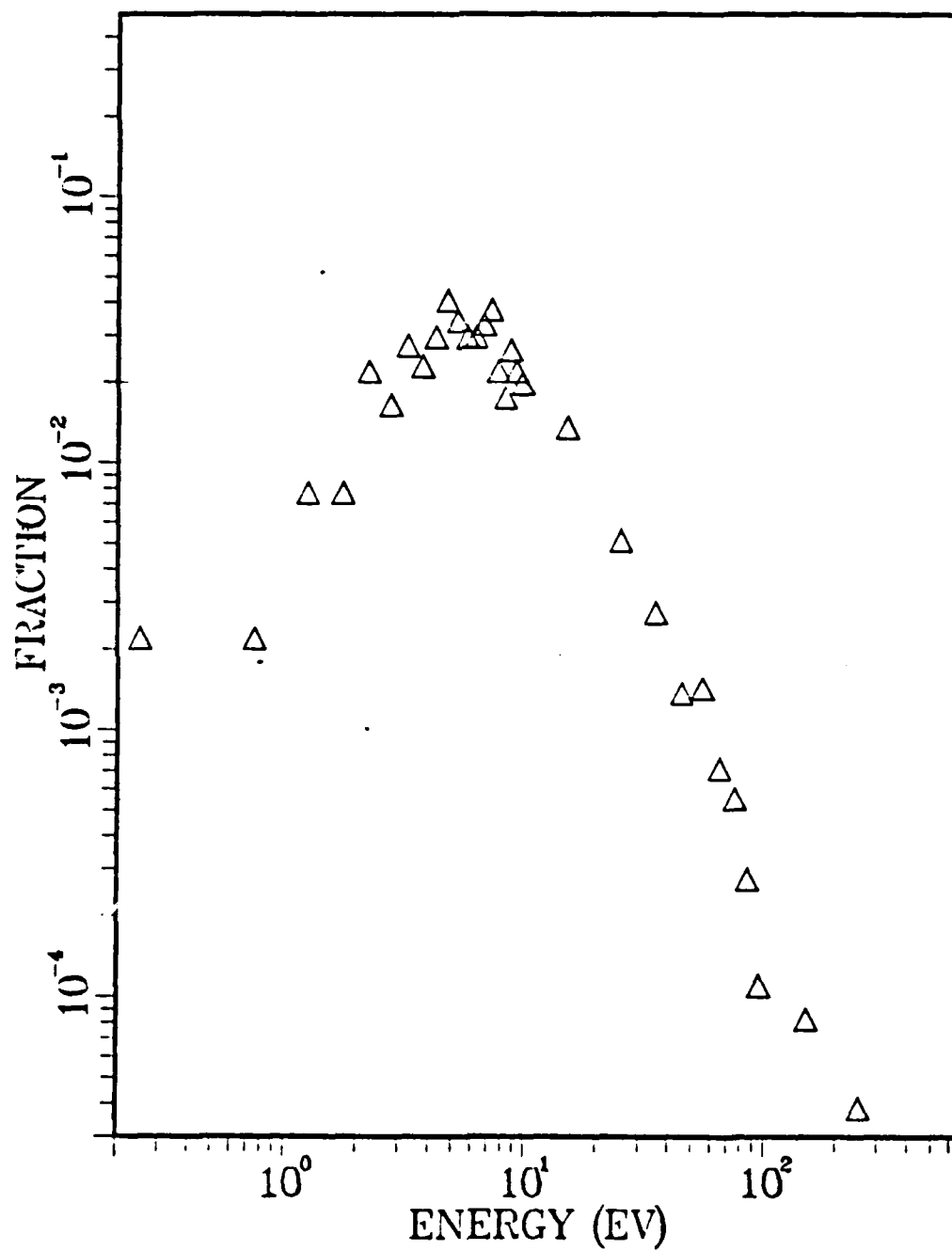## EJECTED ATOM ENERGY DISTRIBUTION

Fig. 43. Log-Log ejected atom energy distribution from clean molybdenum assuming 2 keV argon ion

LIST OF REFERENCES

1. Grove, W.R., Trans. Roy. Soc. (London) v.142,p. 87, 1852.

2. Goldstein, E., Verh. Dtsch. Phys. Ges., v. 4, pp. 22-37, 1902.

3. Plücker, J., Ann. Phys. (Leipzig), v.103, pp. 88-151, 1858; v.104, p.113, 1858; v.105, p.67, 1858.

4. Penning, F.M. and Moubis J.H.A.,"Cathode Sputtering in a Magnetic Field", Koninkl. Ned. Akad. Wehenschap. Proc.,v. 43,pp. 41-56, 1940.

5. Stark, J., Z. Elektrochem., v.14, p.752 1908; v.15, p.509, 1909.

6. A. Von Hipple, E. Blechschmidt: Ann. Phys. (Leipzig), v.80, p.672, 1926; v.81, p.999, 1926; v.86, p.1006, 1928.

7. Kelly, R., Radition Effects, v.32, p.91, 1977.

8. Kingdon and Langmuir, Physical Review, v.20, p.107, 1920; v.21, p.210, 1923; v.22, p.148, 1923.

9. Kewell, F., "Radiation Damage Theory of High Vacuum Sputtering", Physical Review, v.97, pp.1611-1619, 1955.

10. Kewell, F., Physical Review, v.87, p.160, 1952.

11. Harrison, D.E.Jr., "Theory of the Sputtering Process", Physical Review, v.102, p.1473-1480, 1956.

12. Wehner, G.K., "Controlled Sputtering of Metals by Low Energy Hg Ions", Physics Review, v.102, p.690-704, 1956.

13. Silsbee, R.H., "Focusing in Collision Problems in Solids", Journal of Applied Physics, v.28, pp.1246-1250, November 1957.

14. Thompson, M.W., "The Energy Spectrum of Ejected Atoms During High-Energy Sputtering of Gold", Philosophy Magazine, v.18, pp.337-414, August 1968.

15. Thompson, M.W. and Nelson, R.S. , "Atomic Collision Sequences in Crystals", Proc. Royal Society, v.A259, p.458, 1961.

16. Robinson, M.T. and Oen, O.S., "The Channelling of Energetic Atoms in Crystal Lattices", Applied Physics Letters, v.2, pp.30-32, 1963.

17. Davies, J.A., McIntyre, J.D., Cushing, R.L. and Lounsbury, M., Canadian Journal of Chemistry, v.38, p 1535, 1960.

18. Sigmund, P.,"Theory of Sputtering I. Sputtering Yield of Amorphous and Polycrystalline Targets", Physical Review, v.184 no.2, pp.383-415, 1969.

19. J.B.Gibson, A.N.Goland, M. Millgram and G.H.Vineyard, "Dynamics of Radiation Damage", Physical Review, v.120, nr.4, pp.1229-1253, 1960.

20. Winters, H.F., "Mass Effect in the Physical Sputtering of Multicomponent Materials", J. Vac. Sci. Technology, v.20 no.3, pp.493-497, 1982.

21. Meyerhoff, D., Computer Simulation Studies of Sputtering From Clean Tungsten and Nitrogen Reacted Tungsten and Molybdenum Surfaces, Masters Thesis, Naval Postgraduate School, Montertey, California, December 1983.

22. Calvenna, J.R. and Schmidt, L.D., "Interaction of N_2 with (100) W", Surface Science, v.22, p.365, 1970.

23. Adams, D.L. and Germer, L.H., "Adsorption on Single Crystal Planes of Tungsten", Surface Science, v.27, p.21-34, 1971.

24. Griffiths, K., Kendon, C., King, D.A. and Pendry, J.B., "Adsorbate Induced Contracted Domain Structure: Nitrogen Chemisorbed on W(001)", Physics Review Letters, v. 461, pp. 1584-1587, 1981.

25. Harrison, D.E.Jr., Vine, G.L., Tankovich, J.A. and Williams, R.D.III, "Simulation of Inert Gas Interstitial Atoms in Tungsten", Plenum Press New York, pp.427-438, 1973.

26. Harrison, D.E.Jr. and Jakas, M.H., Simulation of the Atomic Collision Cascade, Radiation Effects, v. 91, pp. 263-267, 1986.

27. Huber, K.P. and Herzberg, G., Constants of Diatomic Molecules, 1st ed., Van Nostrand Reinhold Company, 1979.

INITIAL DISTRIBUTION LIST

NO. COPIES

1. Defense Technical Information Center
   Cameron Station
   Alexandria, Virginia 22304-6145

   2

2. Library, Code 0142
   Naval Postgraduate School
   Monterey, California 93943-5000

   2

3. Dr. Don E. Harrison, Jr. Code 61Hx
   Department of Physics
   Naval Postgraduate School
   Monterey, California 93943-5000

   4

4. Department Chairman, Code 61Sq
   Department of Physics
   Naval Postgraduate School
   Monterey, California 93943-5000

   2

5. LCDR Stephen M. Webb
   303 E. Charlotte St.
   Sterling, Virginia 23452

   2

END

11-86

DTIC